

Control of the main engine

CONTROL OF THE MAIN ENGINE

Control of the main engine speed while on passage, and on standby when leaving and entering port was normally from the bridge via the engine telegraph. However, during *MSC Napoli's* passage from Felixstowe to Antwerp, problems were experienced with the main engine governor¹, and it was disconnected. This required engine speed to be controlled by a fuel lever mounted on the side of the engine, which was an emergency method of operation.

A technician was not immediately available to repair the governor in Antwerp. Following discussions between the master, chief engineer and a technical superintendent which included the consideration of the expected adverse conditions in the English Channel, it was decided that it was safe to sail without an operational main engine governor and to arrange for a technician to attend in Sines. The master and deck officers were made aware that control of the engine was now from the engine room and they could order change of engine speed via the wheelhouse engine telegraph. The master assumed that control of the engine was now from the ECR and, as this was not an uncommon practice on older ships, the master did not consider it necessary to inform the pilot when entering or departing Antwerp.

Although the vessel had an Unmanned Machinery Space (UMS) capability her engine room had been continually manned in port and at sea during the two months before the accident. The minimum watch complement consisted of an engineer officer and an engine rating.

On leaving the River Schelde engine speed was slowly increased to 82 RPM, which normally produced a speed of 19 knots. When the ship started to pitch as the seas increased overnight, the engine speed began fluctuating as the propeller began to cavitate. In order to prevent the engine from over-speeding and tripping, the chief engineer ordered the watch engineers to stay close to the engine fuel lever so they could react quickly to the fluctuations in engine speed. By early morning the watch engineers were continually adjusting the fuel lever as the propeller load reduced and the engine revolutions increased as the vessel pitched.

¹ The main engine speed governor was an ABB Dego II, electronic speed control system. The speed of the engine is picked up from the flywheel or the crankshaft and sent to the governor. The system will compare the speed setting with the speed setting value, and will make any necessary adjustments via the fuel rack position. The governor derived engine speed is also used for main engine monitoring and control.

At about 0600 the watch engineer informed the chief engineer that the engine revolutions were fluctuating wildly and a lower average RPM was required to prevent the engine from tripping. The master was informed of the need to reduce speed to which he agreed after he had assessed the situation from the bridge. The fuel lever was then adjusted to a setting equating to an engine speed of about 71rpm, and a vessel speed of about 17 knots.

At about 0800, the engineer charged with monitoring the setting of the fuel lever "screwed down" the lever in a position which had generally produced an average engine speed of 71rpm. He then left the engine to undertake routine maintenance in other areas of the engine room.

Crew details

VESSEL MANNING

MSC Napoli was conventionally manned with a master, chief, second, and third officers. The officers in the engineering department comprised the chief engineer, first, second, and third assistant engineer officers, plus an electrician. The crew consisted of seven deck, five engine and three galley ratings. There were also two officer cadets onboard the vessel. Details of the ship's senior officers were:

Master

The master was a Bulgarian national and initially served in the Bulgarian naval fleet from 1983 to 1991. He joined his first merchant navy vessel, a bulk carrier, in 1992. After sailing on various vessel types as a third and second officer, he was promoted to chief officer on container vessels in 1998. He had sailed as chief officer on *MSC Napoli* in early 2002 and was promoted to master the same year. He joined *MSC Napoli* in late November 2006.

Chief officer

The chief officer was a Romanian national. He first went to sea in 2000 as a deck cadet with a contract with Zodiac Maritime. He was promoted to third officer in 2001 and, before joining *MSC Napoli*, he had completed six contracts on board bulk carriers and container vessels, as a third and second officer. He joined *MSC Napoli* in early November 2006 for his first contract as a chief officer and had received a three day familiarisation handover period with his predecessor.

Chief Engineer

The chief engineer was a Bulgarian national. Following graduation from a naval academy, he joined his first merchant ship in 1984 and had sailed on various ship types as an engineering officer. He was promoted to chief engineer in 2000 and joined *MSC Napoli* in October 2006.

Conclusions of metallurgical tests

**SUMMARY, RECOMMENDATIONS, OPINION AND
CONCLUSIONS IN RESPECT OF TWENTY-ONE SAMPLES
REMOVED FROM THE FORWARD HALF OF THE CONTAINER
SHIP mv MSC NAPOLI**

**Client:
Marine Accident Investigation Branch
First Floor
Carlton House
Carlton Place
Southampton
SO15 2DZ**

**THE TEST HOUSE (CAMBRIDGE) LTD REPORT REFERENCE: T71927S1
REPORT DATE: 1 April 2008**

1. INTRODUCTION

The Test House had been instructed by the Marine Accident Investigation Branch (MAIB), to examine and test a set of eighteen samples removed from the forward half of the stricken container ship mv MSC NAPOLI. The factual findings from the laboratory work, which had been completed to a protocol agreed with owners and charterers, had been published separately in The Test House (TTH) laboratory report reference T71927. The contents of the engrossed factual laboratory report had also been provided to the metallurgical experts representing the vessel owners and charterers.

A further three samples, which had been removed from the forward half of the ship by the Vessel Charterers, were also examined by TTH. The additional three samples were examined under TTH job number T80157 as instructed by Charterers, but with later inputs into the work scope from both Owners and TTH acting for MAIB.

The content of this expert's report, which summarises the two earlier referenced sets of laboratory test data and observations made during attending the forward half of the vessel at Harland and Wolff on 23 August 2007 and 5 February 2008, is prepared in confidence for the MAIB only.

2. SUMMARY

- 2.1** Inspection, at the Harland and Wolff dry-dock, of the transverse breakage site in the vessels forward recovered half identified no obvious visually apparent corrosion wastage of the steel structure. The transverse breakage site also appeared to be essentially free from significant visually apparent fatigue cracking damage.
- 2.2** The visually apparent fracture path in steel plating appeared to be largely ductile in nature. The breakage also included fracture through the throats of fillet welds attaching internal structural members, and this was particularly so at sites of discontinuous longitudinal stiffening.
- 2.3** To confirm the correctness of construction materials and verify the quality and size of construction fillet welds, a series of samples were removed to represent both the parent steel plating and construction welding. The sample set specifically included pieces from areas exhibiting characteristic differences in either the visually apparent mode of fracture or the apparent weld size and detail.
- 2.4** The steel plating used in construction of the vessel, we were advised, was of either Grade A or the tougher and stronger Grade AH32. Twelve samples from parent steel plates were chemically analysed and their conformity to specified grades reviewed.
- 2.5** The population of steel plates include a number of parent steel casts, all of which appeared to be silicon killed aluminium treated and consistent with high quality hot metal practice type virgin steel. The Grade A steel casts had been produced as plain carbon steel, in contrast with the AH32 steel casts which were of Carbon-Manganese type. The analysis of three pieces (PTF2 Floor, PTFL3 Tank Top and PTFL3 Floor) was consistent with the higher strength Grade AH32 material having been substituted for the specified Grade A. In the case of the CL5 girder, a plain carbon steel Grade A type material had been substituted for what should have been a stronger and tougher AH32 material.
- 2.6** The tensile tests of the parent steel plates also confirmed that some grade substitution had occurred in the build process, and the tests results followed those of the analysis findings. Three samples (PTF2 Floor, PTFL3 Tank Top and PTFL3 Floor) were over strength for the specified grade A, but met the requirements of the stronger AH32 grade. The CL5 girder sample exhibited a proof stress of only 254 N/mm^2 , which failed to meet the minimum AH32 specified proof stress of 315 N/mm^2 in the specified transverse test direction. The Ultimate Tensile Strength (UTS) of the CL5 girder plate, however, met the higher AH32 minimum UTS in both test directions

- 2.7** The Single set of Charpy toughness specimen removed from the PBS8 piece just met the minimum AH32 grade toughness requirements at the specified test temperature of zero degrees C. The significantly higher prevailing metal temperature at the time of the casualty would, however, have given a greater margin on toughness than was implied by the laboratory test completed.
- 2.8** Thickness measurements recorded for the first fourteen pieces received by the laboratory were generally in line with specified requirements, and the sample PTF2 transverse floor plate was confirmed to contain the additional 4mm of thickness requested by original owners.
- 2.9** Weld metal hardness characterisation values from the first batch of samples appeared reasonably consistent and were in the general property range we would expect them to be. A number of joints exhibited a small difference in average values for the included welds and some exhibited possible evidence of casualty related strain damage (work hardening).
- 2.10** The more detailed hardness surveys completed on the Charterers three samples identified a wide range of both weld metal and Heat Affected Zone (HAZ) hardness, the recorded values reflecting the apparent wide differences in the apparent welding procedures and heat input in particular. One weld toe HAZ in sample PBS21-B included two hardness readings that were over HV350. The presence of such apparently high hardness readings and an apparently earlier HAZ suggested that the joint had been locally repositioned using an unacceptable weld procedure.
- 2.11** The two cruciform type tensile test specimens produced respectably high weld metal UTS values. The value obtained for the CL15 piece was the highest, and this had been achieved even though the fractured weld metal of this specimen exhibited a significant volume of worm-hole type root porosity.
- 2.12** The fillet welding in the original sample set of eighteen pieces appeared variable in terms of its profile and weld sizes at a given joint. All fillet welds exhibited leg lengths greater than the minimum blanket specified size of 5mm. Some fillets, in samples from pieces PTFL3, CL5, ST11, CL15, SLG16 and SLG17, were potentially very marginally under the minimum location specific required size. The MAIB is recommended to review the aspect and implications in respect of the reported weld sizes with its Naval Architects
- 2.13** Within the original sample set of eighteen pieces a number of structural joints were found to have been either repositioned or locally weld repaired. The samples containing repositioned joints or local weld repairs comprised pieces PTFL3, STL7, STL11, SB14, and SLG16.

2.14 Visual or metallographic evidence of joint repositioning or local weld repairs was apparent in all three of the Charterers additional three samples SG1-19, SG1-20 and BPS21.

2.15 Though the bulk of the plate fractures were entirely ductile in nature, some evidence of fast running brittle fracture was apparent in the two fractures contained within sample PBS8. The Charpy toughness of the PBS8 parent steel plate met the AH 32 minimum requirement at a test temperature significantly lower than would have prevailed at the time of the casualty; consequently it is likely that the rate of loading was the fracture mode determining issue at this vessel location. The fracture at this location was also thought to have followed critical structural failures at other locations of the ship.

2.16 The samples examined were confirmed to be largely free from significant fatigue cracking. A definite short sub-critical fatigue crack was confirmed to have originated from the lightening hole in sample PTF3. A number of other incipient and shallow probable fatigue cracks were present in a number of the macro specimens. The cracks were not considered to be significant, they could not be accurately aged and arguably could have originated post casualty.

3. CONCLUSIONS DISCUSSION AND OPINION

Based on our limited inspections of the forward half of the MSC NAPOLI at the Harland and Wolff dry-dock, we concluded that at the location of transverse fracture the vessel was visually free from both significant corrosion wastage and fatigue cracking. The detailed laboratory examination of both the original eighteen samples and an additional three Charterers samples subsequently removed from the vessel, served to further confirm a freedom from both significant corrosion wastage and fatigue cracking at the time of the casualty.

We are not, unfortunately, able to identify the initiation site, or sites, of the vessels critical structural failure, and similarly our inspections and tests have not identified an obvious cause of the shell plate buckling collapse and fractures.

The vessels plating was found to be largely as specified, or better, in terms of grade and strength, and there was no evidence to suggest that the construction steel lacked the necessary toughness.

The fillet welding of internal structural members appeared variable in terms of its depositional procedure, profile and achieved weld sizes. Local weld repairs or repositioning of structural joints was apparent in five of the original samples and in all three of the Charterers samples. The age of the repositioning or repairs could not be established in the

case of five samples and they could, consequently, be associated with original shipyard construction welding.

Three of the samples did, however, exhibit evidence consistent with the repairs or joint repositioning having been completed after a period of post build service of the ship. Piece STL11 exhibited a fatigue crack that had initiated from a region of weld metal exhibiting pre-existing centre bead segregation, or liquation type hot cracking. The lower fatigue portion of the crack, by contrast, contained an in-situ corrosion product consistent with its formation in a marine environment. Collectively, the evidence suggested that a solidification defect had been present in the throat of the original construction weld. The crack had grown by a mechanism of fatigue and been open to the elements, during which time the lower crack regions had suffered corrosion. The crack had then been partly excavated and a capping weld run applied over the previously open and corroded crack. The tank top connection in piece SG1-20 exhibited both repositioning of the weld and local disturbance of the tank coating, which was again consistent with the repositioning or repairs having been completed some time after the vessel had entered service. The weld in bottom plate sample BPS21 also exhibited evidence of repair welding or stiffener repositioning after a period of in service corrosion. The original fillet weld had initiated lamellar tearing in the bottom plating HAZ, after which the joint had been repositioned and re-welded. After the repositioning, the weld root area had suffered a period of heavy corrosion, before the joint root was again sealed with an additional stringer bead of weld metal.

The apparent widespread evidence of local repair welding, some of which was clearly and demonstrably post build, would suggest that there had been earlier local structural integrity problems and issues in respect of fillet weld integrity in particular. The number of repositioned or repaired fillet welds and the apparently indiscriminate local use of vertically-up positional welding were similarly seen as inconsistent with original construction practice.

Though there was evidence of post delivery repair welding to structural members, it was not possible from the metallurgical evidence, to establish an age or the period of vessel ownership during which the repairs had been completed.

The apparent need to complete structural weld repairs after the ship had entered service suggested that there were possible design and local structural joint loading issues. The cracking should have flagged-up a possible structural weakness and represented an opportunity, or opportunities, to consider the suitability of the basic design and local structural integrity. The apparent absence of any records in respect of the weld repairs would appear to represent both a possible reporting deficiency and a missed opportunity to identify any potential local design weakness.

Though not thought to be casualty critical, a number of the fillet welds examined macrographically were found to be potentially very marginally under the specified minimum required size. The MAIB are consequently advised to review the aspect of fillet weld sizes with its Naval Architects.

The cross cruciform joint strength was found on test to be significantly better than we would have expected to see in shipyard construction fillet welding, and the weld strength was not significantly compromised by the presence of widespread welding defects. This latter observation in respect of the achieved cross joint strength may in reality have negated any small potential shortfall in weld size.

We conclude that the vessels failure was not attributable to any identifiable material or metallurgical deficiencies or issues and that steel work was thought to have been in good order, in terms of freedom from both corrosion wastage and significant fatigue cracking, at the time of the casualty. The MAIB is consequently advised to look for a cause of the casualty in the vessels Naval Architecture, operation, or both.

Det Norske Veritas report on load and strength assessment



TECHNICAL REPORT

DET NORSKE VERITAS AS

MARITIME TECHNOLOGY AND PRODUCTION CENTRE

MSC NAPOLI

REPORT

LOAD AND STRENGTH ASSESSMENTS

18 JANUARY 2007 INCIDENT

REPORT No. 2007-1928

REVISION No. 00

DET NORSKE VERITAS AS



TECHNICAL REPORT

Date of first issue 2007-11-29	Project No.: 359NQ025
Approved by: Liv A. Hovem, Head of Department Geir Dugstad, Head of Department	Organisational unit: MTPNO360 MTPNO870
Client: Technical Director DNV Maritime	Client ref.: Olav Nortun

DET NORSKE VERITAS AS
Maritime Technology and
Production Centre
Technical Solutions
Veritasveien 1
1322 Høvik
Norway
Tel: +47 67 57 99 00
Fax: +47 67 57 99 11
http://www.dnv.com
Org. No: NO 945 748 931 MVA

Summary:

This report summarises the main assumptions and findings from the direct load and strength analyses of the MSC Napoli 4400 TEU container vessel carried out by DNV Maritime/Section for Hydrodynamics, Structures and Stability

The basis for the investigation is

- the environmental data in the English Channel relevant for the sea states around the time of the incident 18th January, 2007
- the still water loading condition from the onboard loading computer
- design drawings provided by the builder
- DNV computer analyses for wave loads and hull strength

The analyses estimate a possible load range for the vertical bending moment and shear force in way of the engine room bulkhead and the corresponding structural hull capacity range. Hydrodynamic analysis tools have been used for the wave load assessments (WASIM) and non-linear FE models (ABAQUS) for the structural capacity estimates.

From the detailed computer analyses it is found that hull cross sections in way of the engine room area (# 81 to # 88) develop a very localized structural collapse pattern for high loads. Moreover, the collapse pattern is found to extend across the whole cross-section, starting around # 81 in the bottom area, moving slightly forward across the sea chest area and ending high up in the ship side, just aft of the engine room bulkhead (#88). The final localized collapse pattern is documented to be the result of a progressive collapse mechanism, starting with initial buckling in the bilge area in way of the engine room with subsequent collapse spreading into the bottom area and upwards into the ship side. The calculated collapse pattern is very similar to the one observed onboard the vessel.

The large localized plate deformations are likely to lead to plastic strains and plate rupture followed by water ingress and flooding of compartments. It is also documented that the overlap in load and capacity is very narrow indicating that such a failure scenario has a very low probability of occurrence for the sea states as documented at the 18th of January 2007. Moreover, by screening available wave statistic relevant for the English Channel during the last years it can be concluded that such sea states are very rare. This in sum reflects a very low probability for such events to take place in the future.

Report No.: 2007- 1928	Subject Group: H1	Indexing terms	
Report title: MSC Napoli, Load and Strength Assessments - 18 January 2007 incident		Key words Container ship Extreme Loads Hull Girder Strength Collapse	Service Area
			Market Sector
Work carried out by: Gaute Storhaug, Octavi Sado, Jon Kippenes, Michal Moczulski, Eivind Steen		<input type="checkbox"/> No distribution without permission from the client or responsible organisational unit (however, free distribution for internal use within DNV after 3 years) <input type="checkbox"/> No distribution without permission from the client or responsible organisational unit. <input checked="" type="checkbox"/> Strictly confidential <input type="checkbox"/> Unrestricted distribution	
Work verified by: Thor Hysing, Tom K. Østvold, Håvard Austenford, Eirik Byklum, Frode Kåmsvåg, Torbjørn Lindemark, Ivar Håberg			
Date of this revision: 2007-11-29	Rev. No.: 00	Number of pages: 34	

© 2007 Det Norske Veritas AS
All rights reserved. This publication or parts thereof may not be reproduced or transmitted in any form or by any means, including photocopying or recording, without the prior written consent of Det Norske Veritas AS.

<i>Table of Content</i>		<i>Page</i>
1	INTRODUCTION	2
1.1	General	2
1.1.1	Objective	2
1.1.2	Input data and main assumptions	4
1.1.3	Method	4
1.1.4	Report content	5
2	SHIP MAIN DATA	6
2.1	General	6
2.2	Main Dimensions and General data	6
3	METHOD OF ANALYSES - OVERALL.....	8
4	WAVE LOAD ANALYSIS.....	9
4.1	General	9
4.2	Wave load sensitivity study	10
4.3	Hull girder load assessment for the incident	11
4.3.1	Ship loading condition – onboard loading computer	11
4.3.2	Environmental data – definition of sea states for wave load analyses	11
4.3.3	Wave load assessments	13
4.3.4	Whipping effects	14
4.3.5	Load results summary	15
5	LINEAR STRESS ANALYSES.....	17
5.1	Basic model description	17
5.2	Results	18
6	NON-LINEAR ANALYSES – COLLAPSE AND FAILURE ASSESSMENTS.....	21
6.1	Model description	21
6.1.1	Mesh density and properties	22
6.1.2	Geometrical shape imperfections (tolerances)	25
6.1.3	Material properties and yield stress variations	26
6.1.4	Load applications	28
6.2	Results	28
6.2.1	General	28
6.2.2	Hull girder capacity	29
6.2.3	Hull girder failure mechanism	30
7	SUMMARY	32
7.1	General	32
7.2	Discussion	33
	REFERENCES.....	34

1 INTRODUCTION

1.1 General

On request by DNV Maritime/Technical Director, the Section for Hydrodynamics, Structures and Stability has carried out a wave load and strength assessment of the 4400 TEU Container Vessel, MSC Napoli, DNV id. no. 24568.

The background is the incident that took place in French waters 70km south-east of the Lizard Point in the English Channel at about 10.30 am, on the 18th of January 2007.

1.1.1 Objective

The objective of the present documented work has been by theoretical estimates of induced loads and structural strength of the vessel to identify a possible cause of the incident, leading up to the final failure mechanism as illustrated on the pictures taken at open sea, see Fig.1.1.



Fig. 1.1 Structural damage in ship side. Pictures taken 18th of January 2007 after ship has been abandoned. (with permission from Gargolaw)

The first step was to go through ship records to see if any relevant information from previous incidents could be of interest. The most relevant information found was a grounding accident on the Helene Mar Reef in Singapore Strait in 2001, with damages in the forward half of the vessel. This case was assessed to see if there could be possible links to the present incident. Simple grounding simulations and theoretical strength assessments were carried out concluding that no such links were likely and the 2001 grounding was ruled out as a possible implicit cause to actual 2007 incident.

Other failure scenarios related to fatigue, engine vibrations etc. have been evaluated but not found relevant for this incident and therefore not documented herein.

Documented scenario:

From the pictures taken of the MSC Napoli at sea, Fig.1.1, it can be seen that the localized damage extends vertically at both starboard and port sides. Moreover, the change of the deck line slope at the engine room bulkhead, as marked up in Fig.1.2, implies that the bottom structure in this area must have shortened significantly in the longitudinal direction in order for this hull girder rotation (hinge) to develop. Such a bottom shortening is likely to be the result of buckling and collapse of longitudinally compressed elements in this region.



Fig. 1.2 Structural damage in Ship side illustrating the change of deck slope at engine room bulkhead. (with permission from Gargolaw)

The analysis procedure for the strength assessment documented herein has the following steps:

- i) Assess the ship hull loads at the time of the incident using hydrodynamic wave load programs
- ii) Assess the hull girder stress levels and ultimate capacity with focus on identifying collapse failure mechanism (structural finite element programs)
- iii) Compare i) and ii) for possible loads exceeding the capacity

The main focus is on the hull sections in way of the engine room area, from around sea chest area (# 81) to engine room bulkhead (#88) since this area covers the collapsed hull plates with cracks, as seen and documented in Fig.1.1 above.

1.1.2 Input data and main assumptions

An important assumption and input for the analyses has been the actual loading condition and longitudinal mass distribution for the vessel at the time of the incident. In this respect, the data from the onboard loading computer as provided by MAIB-UK, has been used, ref./1/.

Environmental data like wave heights, wave periods etc. at the location and time of the incident also constitutes an important input to the wave load simulations. Thus a broad collection of data from different sources such as the media, Ocean Systems Incorporated (OSI), Argoss, UK Met office and others was initiated.

Based on these data and considering variation of the reported parameters, two relevant sea states were chosen (“high” and “low”) and both analysed with respect to hull girder sectional loads in way of the engine room area (#88), see Chapter 4 for more details.

The basis and main assumptions for the linear (SESAM) and non-linear (ABAQUS) structural finite element (FE) models are

- scantlings with “as built” dimensions
- no corrosion margins deducted
- FE model made according to drawings provided by builder
- normal fabrication tolerances implemented as geometrical imperfections in the non-linear structural analyses (ABAQUS)

1.1.3 Method

The computer analyses presented herein have three main elements:

- i) Hydrodynamic wave load analyses using DNV’s tool WASIM, ref./2/
- ii) Global FE linear stress analyses of complete ship with a standard element mesh for most of the ship hull, and with a fine mesh model in engine room area (#64 - #106), see Fig. 5.1 and Fig. 5.2. The linear stress analyses is done using DNV’s SESAM FE system, ref./2/
- iii) Advanced non-linear stress and ultimate capacity analyses: Global FE model with non-linear (ABAQUS) sub-model i.w.o. engine room (#79 - # 92), ref./3/.

It is realized that it is difficult to assess the maximum acting wave load and the corresponding hull capacity accurately considering all the uncertainties and variations in input data. In particular this is true in relation to environmental data like wave heights, wave periods etc. Therefore, the present approach is to assess ranges of global loads and hull capacities within which the MSC Napoli most likely has been operated around the time of the incident.

1.1.4 Report content

The report contains the following sections:

- Chapter 2 - Ship main particulars
- Chapter 3 – Overall analysis methodology. A brief listing and description of the methods and computer models developed and analysed is given. This includes both hydrodynamic wave models, structural FE models and the load transfer between them.
- Chapter 4 - Wave load analyses - WASIM
 - o Chap 4.2 - A wave load sensitivity study is presented. The purpose is to investigate the MSC Napoli general wave response properties under variable assumptions with respect to wave characteristics and ship mass distributions.
 - o Chap 4.3 - Summary of wave load analyses for two specific defined sea states, Case 1 “high” and Case 2 “low” respectively, both considered relevant for the actual incident in the English Channel on the 18th of January 2007. Main results are the total load range embracing both Case 1 and Case 2 sea states.
- Chapter 5 - Summary of the Global FE model (SESAM) and linear response analyses of the hull with focus on the stress levels in way of the engine room area, # 64 to # 106.
- Chapter 6 - Advanced structural collapse analyses of ship hull using a non-linear FE model (ABAQUS) for identifying possible buckling triggers, stress redistributions, progressive collapse and ultimate capacity limits. The main output is a hull girder ultimate capacity range to be compared against the extreme wave load range from Chap. 4.3, and the nature of the collapse localization and failure mechanism developed.
- Chapter 7 - Overall summary, discussions of main findings

2 SHIP MAIN DATA

2.1 General

The basis for the computer analyses herein are ship drawing as provided by builder January 2007.

2.2 Main Dimensions and General data

The ship general data and main particulars are given in Table 2.1 and Table 2.2 respectively.

Table 2.1 Ship General and Class data

General	
Vessel Name:	MSC Napoli
Previous vessel names	2001 - 2004 CMA CGM NORMANDIE 1995 - 2001 Nedlloyd Normandie 1991 - 1995 CGM Normandie
DNV ID No.:	24568
Owner:	Metvale Ltd.
Manager:	Zodiac Maritime Agencies Ltd.
IMO No:	9000601
Port of Registration:	LONDON
Flag:	United Kingdom
Signal Letter:	VQBX7
Builder Name:	Samsung Heavy Industries Co. Ltd., Koje Shipyard
Builder Hull No.:	1082
Year of Build:	1991
Deadweight (tonnes):	62277 (4419TEU)
Sister vessels	None
Class Data	
Class built to	BV
Date of DNV class assignment:	2002-09-23
DNV Class notation:	✠ 1A1 Container Carrier E0

Table 2.2 Ship Main Particulars

Length over all, L_{OA}	275.6	[m]
Length between perpendiculars, L_{PP}	261.4	[m]
Scantling length	258.31	[m]
Breadth moulded, B	37.1	[m]
Depth moulded, D	21.5	[m]
Block coefficient, C_B	0.609	
Top of hatch coaming above BL	23.3	[m]
Draught, T (scantlings)	13.5	[m]
Draught, T (design)	12.4	[m]

3 METHOD OF ANALYSES - OVERALL

Different analysis tools have been used in order to assess the loads and hull strength. The stability program system NAPA, ref./4/ has been used for the hydrostatic and still water load assessments while the DNV- WASIM hydrodynamic software package has been used for the wave load assessments, ref./2/. The DNV-SESAM FE program suite has been used for the linear stress analyses, ref./2/, and the non-linear finite element program ABAQUS, ref./3/ for the non-linear collapse, failure and capacity assessments.

A brief description of the adopted methods and computer models developed are given below:

- i) **Still-water loads.** The hydrostatic properties of the vessel are established using the NAPA software suite. The basis is the loading condition logged on the onboard loading computer before the incident, ref./1/.
- ii) **Wave loads.** Wave loads are assessed using the DNV-WASIM hydrodynamic software package, ref. /2/. Wave load ranges are assessed for two set of environmental conditions referred to as Case 1 “high” and Case 2 “low”. Based on these results a total load range is identified, which includes Case 1 and Case 2. Both sea states are considered relevant and based on the available metrological data around the time of the incident. The wave load procedure has two steps:
 - a) **Linear wave load estimates.** This approach follows well established procedures assuming Rayleigh distributed wave loads for the short term statistics. Thus probability distributions for the wave loads at the engine room bulkhead (# 88) are found for the two defined sea states separately.
 - b) **Non-linear load estimates.** For slender ships like container vessels the linear ratio between hull response and wave amplitude is violated due to non-linear effects from large wave amplitudes in interaction with the hull shape. WASIM provides non-linear assessments of the hull bending moment using time series analyses in irregular sea states.
- iii) **Whipping effects.** Ships in severe waves may experience a transient whipping response (2-noded global hull vibration mode) due to flare or bottom slamming. This means that the hull girder may have an extra longitudinal hull bending and shear stress acting on top of the stresses from the regular more slowly varying wave response for a limited time. Whipping effects for the MSC Napoli are not quantified in this report, but considered to be a possible trigger of structural failure.
- iv) **Global FE SESAM model development.** A FE model of the complete vessel is developed including an accurate modelling of the structural arrangement in way of the engine room area # 64 - # 106. Containers and superstructure are included and the hull shape and lines are based on the NAPA model i) above.
- v) **Load transfer to Global FE SESAM model.** Loads from the non-linear hydrodynamic model are transferred to the Global FE model.
- vi) **Analyses of Global FE SESAM model.** Linear stress analyses are carried out for the wave loads from v). Stress plots illustrating the nominal stress flow in way of the engine room are included in this report, see Chapter 5.
- vii) **Development of Global FE ABAQUS model.** A Global FE model with **very fine mesh** in way of the engine room area (# 82 - # 96) is developed by refining the SESAM FE model IV) above.
- viii) **Load transfer to Global FE ABAQUS model** follows the same principle as for the linear Global FE model v) above.

- ix) **Global FE ABAQUS analyses.** The complete global FE model is imported into the ABAQUS program and analysed for non-linear structural response, hull girder ultimate capacity and failure mechanism identification. The Global FE ABAQUS model is analysed by scaling the wave loads until the hull girder collapse limit has been identified. Several non-linear analyses are carried out in order to find a range in the hull girder capacity reflecting possible uncertainties and variations in material yield stresses.

4 WAVE LOAD ANALYSIS

4.1 General

The wave conditions around the time of the incident constitute a significant source of uncertainty. In the present assessments data have been logged and analysed from different sources such as the media, Ocean Systems Incorporated (OBI), Argos and the UK Met office.

The data have been carefully examined and evaluated in order to define realistic environmental parameters to be used as input for the WASIM wave load assessment. These analyses have been carried out in the following steps:

- Chapter 4.2 - Wave sensitivity study: Systematic variation of environmental and ship loading parameters in order to quantify the MSC Napoli general wave response characteristics
- Chapter 4.3 - Hull load assessment applicable for the incident
 - o Chapter 4.3.1 Loading condition at departure River Schelde, Antwerp 17th of January: Description of loading condition as logged by onboard loading computer, ref. /1/.
 - o Chapter 4.3.2 Environmental data – definition of sea states for wave analyses. Two sea states, Case 1 “high” and Case 2 “low” are defined, both considered relevant and based on actual environmental data as reported around the time of the incident 18th of January.
 - o Chapter 4.3.3 Wave load assessments. Wave load ranges of vessel for the two defined sea states Case 1 “high” and Case 2 “low” are documented. A total load range including both Case 1 and Case 2 is defined, Table 4.3.
 - o Chapter 4.3.4 Whipping effects. A discussion of the whipping phenomena in general terms and its relevance for MSC Napoli incident.

4.2 Wave load sensitivity study

The wave load sensitivity study was made in order to quantify the main response characteristics of the MSC Napoli operating under environmental conditions typical for the English Channel with finite water depth effects, wave profile variations, vessel speed variations, etc. The most important findings were:

- i) A wave period of approximately 10 seconds gives the highest vertical bending moment (VBM) at the engine room bulkhead at frame #88. This is close to the actual wave periods reported for MSC Napoli around incident.
- ii) The water depth is a moderately important parameter. VBM is of the order 10% higher at 70 m water depth than at infinite depth (#88). A water depth of around 70 m is representative for the location of the MSC Napoli at the time of incident.
- iii) Assuming an almost uni-directional (long-crested) wave train hitting the vessel gives of the order 10 % higher VBM (#88) than the more normal (short crested) sea. It is not unlikely that a rather uni-directional wave train hit the MSC Napoli.
- iv) The energy concentration in the waves, i.e. the regular wave ($\gamma = 5$) in relation to a more “disturbed” wave ($\gamma = 1$) (γ in JONSWAP wave spectre) is found to increase the wave moment of the order of 15%. From the reported conditions of opposite wind and current directions and considering the shallow water conditions, it is not unlikely that a rather regular wave train hit MSC Napoli.
- v) A ship heading angle against the main wave direction varying between 0 and 15 degree has negligible effect on the VBM (#88). The MSC Napoli had most likely a close to head sea direction around the time of incident.
- vi) A variation of the average speed of 5 knots up-or-down from 11 knots implies approximately a wave load change of the order 10%. The higher speed the higher wave load. The MSC Napoli had most likely an average speed around 11 knots at the time of incident as informed verbally by MAIB.
- vii) In order for realistic wave loads to be assessed on slender container ship hulls, non-linear effects from the ship moving in and out of large waves have to be accounted for. The non-linear effect for a hogging wave condition, i.e. a moment in time where the vessel is positioned with a wave crest around mid-ship area (see Fig. 4.1), reduce the wave loads relative to standard linear methods. For the MSC Napoli this reduction is assessed to be of the order 20-25% for the environmental conditions as typical for the English Channel. The final total wave load range as given in Table 4.3 accounts for these non-linear effects.
- viii) The main effect of longitudinal container mass variations is the change in the still-water moment and not the wave bending moment. This implies that by varying the container mass distributions up or down slightly this may change the still-water moments somewhat, but it will have a negligible effect on the wave loads.

4.3 Hull girder load assessment for the incident

4.3.1 Ship loading condition – onboard loading computer

The loading condition used herein is based on the on-board loading computer data at departure River Schelde Antwerp, ref. /1/. The still-water loads for this loading condition are summarized in Table 4.1 below, giving both the vertical hogging bending moment (VBM_{SW}) and corresponding shear force (VSF_{SW}) at the engine room bulkhead position (#88).

Table 4.1 Still-water loads (NAPA) at engine room bulkhead (# 88)

Loading condition	Still-water moment (MNm)	Still-water shear force (MN)
	Hogging VBM_{SW}	VSF_{SW}
Departure River Schelde, ref./1/	2243	20

4.3.2 Environmental data – definition of sea states for wave load analyses

The wave and environmental conditions around the time of the incident constitute a significant source of uncertainty and the available reports from different metrological offices give rather large variations in data. However, in order to assess wave loads some basic assumptions regarding wave heights, wave periods, water depth, vessel speed etc are needed. Based on a thorough examination of the existing data, judgement of possible sources of uncertainties and using in-house experience in combination with the wave sensitivity output result from Chap. 4.2, two sea states were defined:

- 1) Case 1 “high”
- 2) Case 2 “low”

The complete set of environmental parameters used for each of the two sea states are summarized in Table 4.2 below.

Table 4.2 Definition of sea states; Case 1 “high” and Case 2 “low”

Parameters	Case 1 “high”	Case 2 “low”
Significant wave height ($H_{1/3}$)	9	7
Wave up-crossing period (T_z) (sec)	11	10
Vessel heading (degrees from aft)	180 (head sea)	165
Vessel speed (knots)	11	11
Wave spreading (\cos^n)	8	6
Wave spectra (JONSWAP, γ)	5	1
Water depth (m)	54	73

Case 1 “high” is considered to be a severe environmental condition giving severe global hull loads. In particular, assuming a very narrow wave spreading function (\cos^8) means that almost all wave energy is localized into an uni-directional wave train meeting the vessel in head sea. Moreover, a $\gamma = 5$ in the JONSWAP wave spectrum reflects an energy rich, regular and steep wave profile. A significant wave height of 9 m is high, but not unrealistic for a short duration.

Case 2 “low” represents a less severe set of environmental conditions. By setting the JONSWAP wave spectrum parameter to $\gamma = 1$ (Pierson- Moskowitz spectrum), the wave profile is more “disturbed” and in line with standard class guidelines and international recommendations (fully developed sea). A significant wave height of 7 m is very likely and as reported by different met offices. Moreover, a vessel speed of 11 knots at a 15 degrees angle off head sea is also within the variations as reported.

While the two cases defined might both be realistic according to measured and observed sea conditions, the “high” and “low” states are assumed to be boundaries of the range of likely sea states inducing wave loads on the vessel.

It is emphasized that the sea states used here are based on observed wave conditions relevant for the 18th of January 2007. By screening available wave statistic relevant for the English Channel during the last years it can be concluded that such sea states are very rare.

4.3.3 Wave load assessments

The wave loads for the vessel as presented herein are representative for the ship “frozen” in waves as illustrated in Fig. 4.1. In such a moment in time, typically with a wave crest approximately mid-ship, the aft ship is accelerating vertically upwards out of the waves do to a combined heave and pitch effect. In response to this, the hull girder will set up a significant hogging condition, giving longitudinal compressive stresses in the bottom and bilge area.

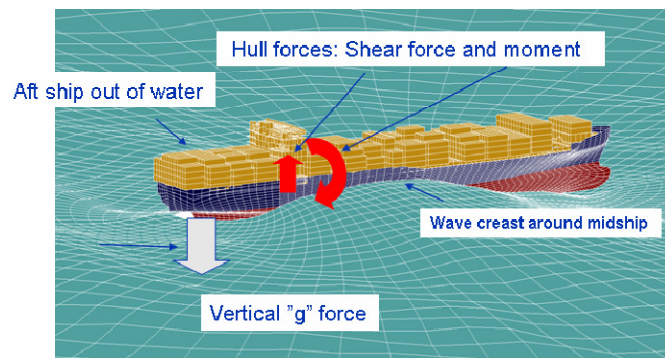


Fig. 4.1 Ship “frozen” in waves in a moment time giving high hull girder hogging loads

The maximum wave loads at the engine room bulkhead are illustrated as probability distributions (Rayleigh) in Fig. 4.2 for the two sea states analysed, Case 1 “high” and Case 2 “low”. It is to be noted that the probability distributions in Fig. 4.2 have been scaled down by 27% and 20 % (Case1, Case 2) according to the non-linear hogging wave effect relative to linear methods. This is done in order to reflect the real life vessel response as closely as possible.

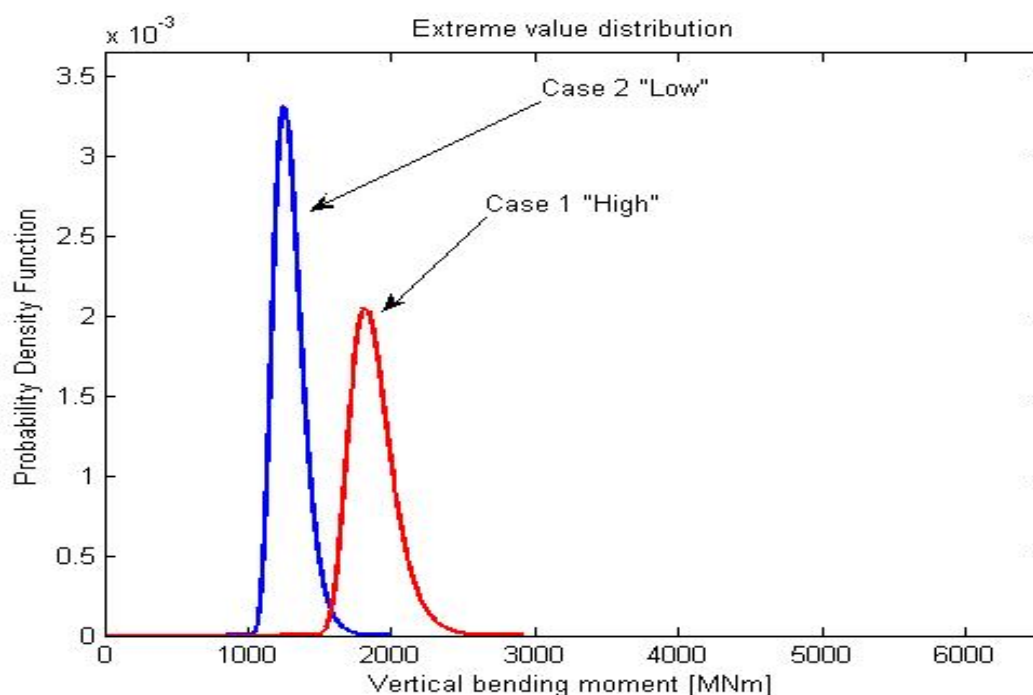


Fig. 4.2 Short term statistics – probability distributions for the vertical wave bending moment (VBM) at #88 for the two sea states Case 1 “high” and Case 2 “low”. Non-linear wave effects are included.

4.3.4 Whipping effects

Possible whipping effects for the MSC Napoli, relevant for the 18th of January incident, have not been assessed theoretically in this report because reliable methods and analyses tools for such evaluations are not available. This status is mainly due to the complexity and randomness of the problem and the theories and software tools are accordingly not fully developed and tested.

The whipping response is a short duration transient vibration effect being the result of the ship slamming against the waves. The vibration period is typically 1 to 2 seconds and this whipping response can last of the order of half a minute or more. The vibration acts on top of the more regular and slowly varying wave response. It can last for several wave periods and thus amplify the stress response for a vessel in a sagging state as well as in a hogging state as the ship moves through the waves.

Whipping response on container vessels have been monitored on actual ships as well as in model tank experiments. All these measurements indicate that whipping is an effect to be considered for slender hull designs. However, the variations and uncertainties are large and for container vessels the additional wave load can typically be in the range of 10% to 50 % or even larger. Fig. 4.3 illustrates schematically how a whipping effect will increase a regular wave load.

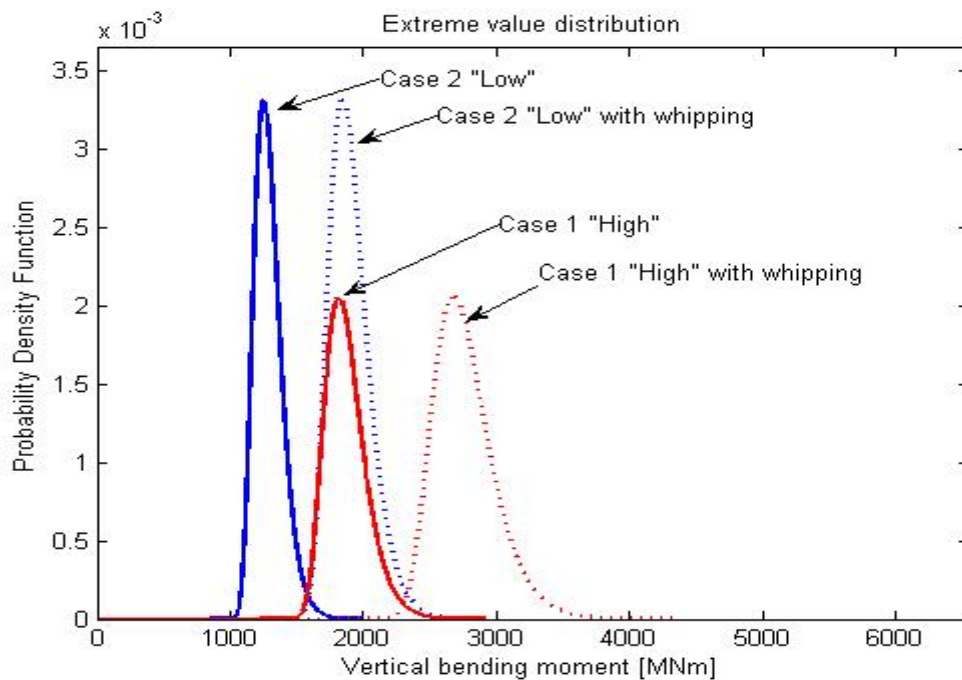


Fig. 4.3 Short term statistics – probability distributions for vertical wave bending moment (VBM) at #88 for the two sea states including a schematic whipping correction. Non-linear wave effects are included.

Full scale measurements and model tank experiments on container vessels have also clearly indicated that whipping effects are strongly vessel speed dependent with higher loads for higher speeds.

Another issue related to the whipping effect is its transient short period (1-2 sec) characteristics and how these dynamic features interact with complex non-linear structural collapse behaviour. Such interaction effects are not assessed in the present analyses as consistent methods are not available.

4.3.5 Load results summary

For the load against capacity comparison a total load range is defined covering both Case 1 “high” and Case 2 “low” sea states. This is done since it is difficult to accurately assess the maximum wave loads due to the relatively large uncertainties in critical parameters such as wave height, wave period, wave steepness, vessel speed, vessel headings, water depth etc.

The total load range defined includes the still-water loading on top of the wave load range. The results are given in Fig. 4.4 in terms of vertical bending moment range at the engine room bulkhead (#88).

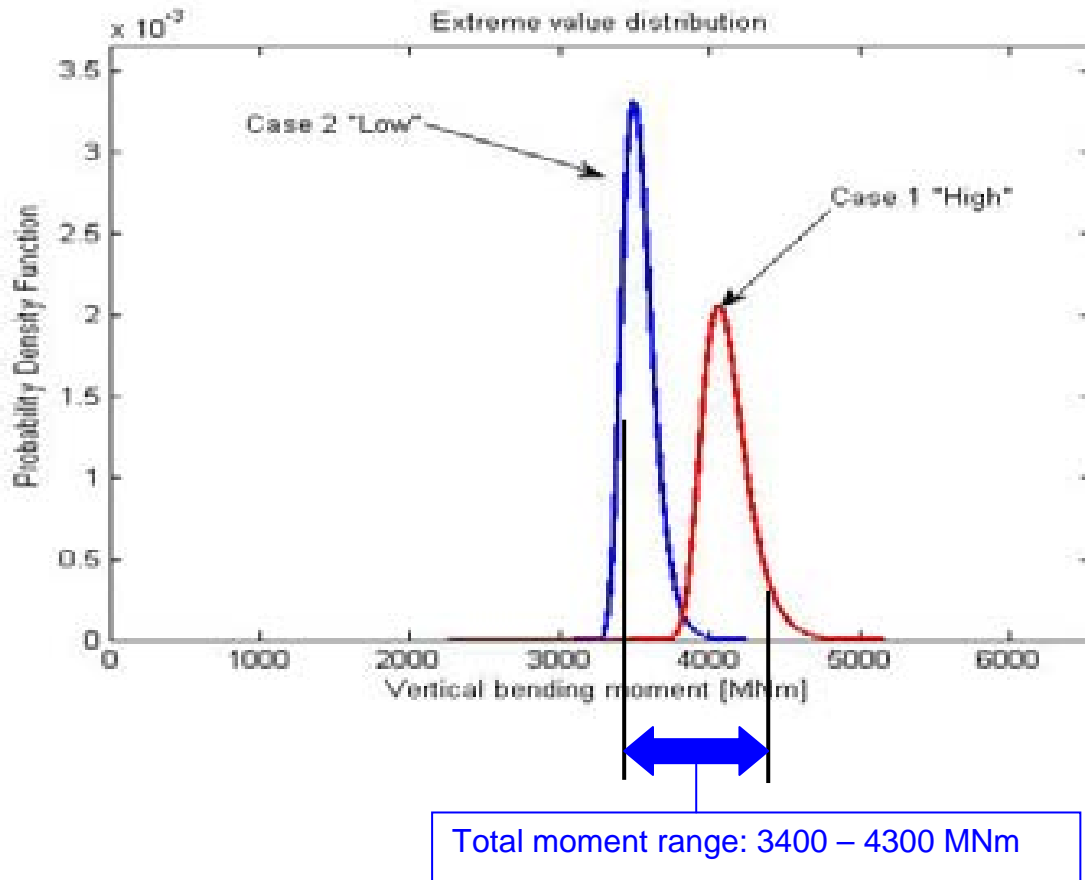


Fig. 4.4 Total load ranges: still-water + wave load (VBM) at engine room bulkhead (#88). Non-linear wave effects are included in all curves while whipping is excluded.

In Table 4.3 the total likely load range is summarized for overview. The total moment range defined includes the likely span of the extreme wave loads assuming Rayleigh distributed short term statistics. For the Case 1 “high” a 10% probability of exceedence value has been used for the upper limit wave load. This limit corresponds to a total moment of 4300 MNm. A similar definition of 10% probability is used for the Case 2 “low” giving a lower bound value of 3400 MNm.

Table 4.3 Total load range at #88; still-water + wave load (no whipping)

Load range	Lowest load Hogging VBM (MNm)	Highest load Hogging VBM(MNm)
Vertical bending moment at # 88	3400	4300

Global shear loads are also assessed corresponding to the VBM ranges. The shear loads are typical in the range 30 - 40 MN for a VBM range of 3400 - 4300 MNm.

5 LINEAR STRESS ANALYSES

5.1 Basic model description

A full global FE model of the MSC Napoli has been made and analysed with special focus on stress assessments in way of the engine room area. The model is shown in Fig. 5.1 and Fig.5.2.

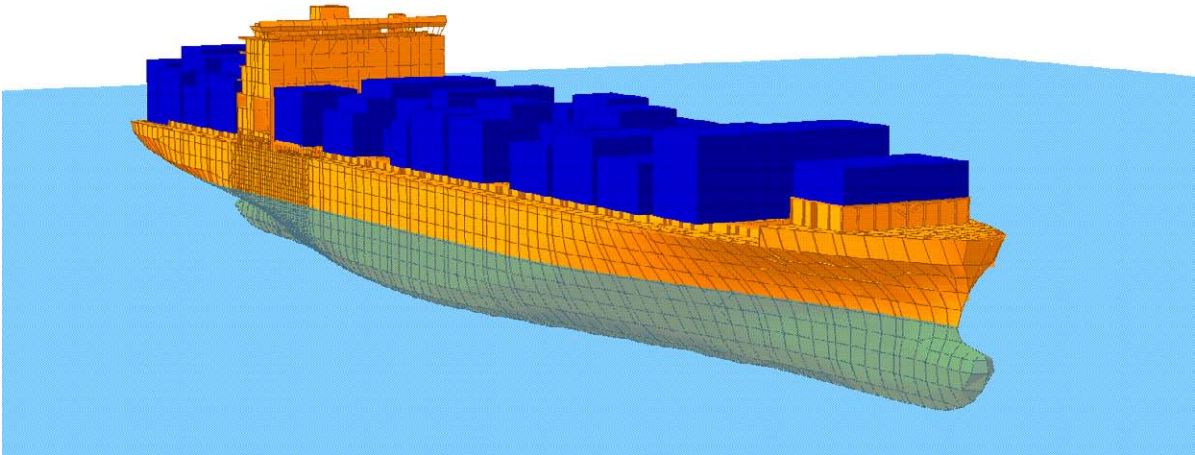


Fig. 5.1 Global FE model of MSC Napoli with fine mesh in engine room area

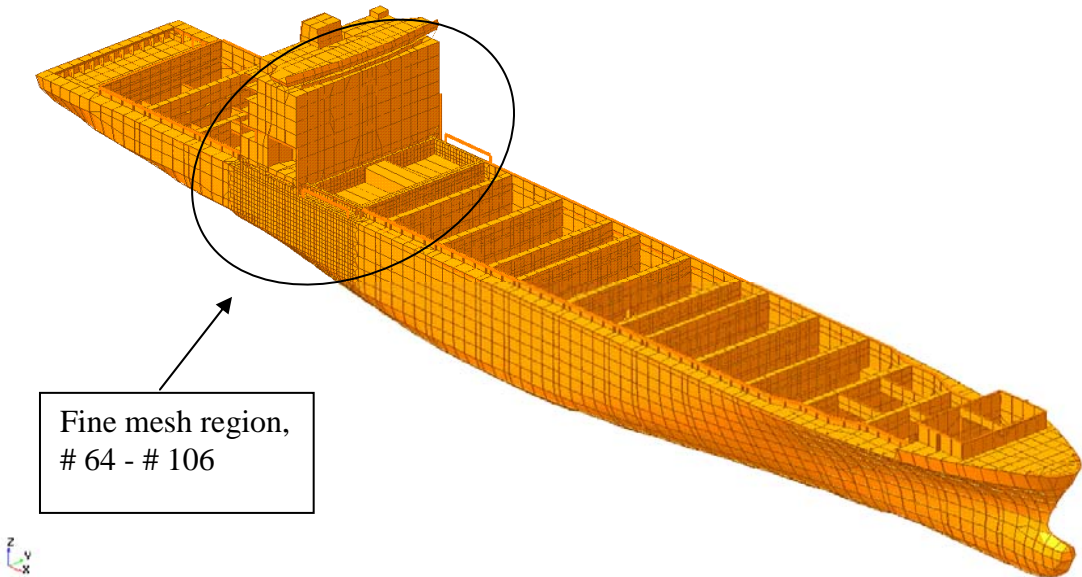


Fig. 5.2 Global FE model of MSC Napoli with fine mesh in engine room area

Global FE model:

The global FE model is made using the DNV - SESAM software package and PATRAN-PRE is used as the main modelling tool, ref./2/.

The general plating is represented by 3 and 4 node shell elements and the stiffeners by 2-node beam elements. Containers are modelled as solid boxes and it is ensured that there is no stiffness interaction between the containers and the hull structure, i.e. the containers follow the hull deflections without influencing on the hull stiffness. Thus, a consistent transfer of self-weight and acceleration forces from containers into the hull structure is provided.

The total number of degrees of freedom (dof) are close to 190 000.

Load transfer and analyses:

Loads acting on the vessel for a fixed position in the waves, as illustrated in Fig 4.1, are transferred from the WASIM hydro model.

5.2 Results

For stress result presentations, the reference load levels according to Table 4.3 are used. The stress results shown in Fig. 5.3 and Fig. 5.4 are valid for a vertical bending moment (VBM) at #88 of 3300 MNm. Similar plots are given in Fig. 5.5 and Fig. 5.6 for a VBM of 4600 MNm

All stress plots are presented against the material yield values of ± 315 MPa (grey), where red (tension) and dark blue (compression) represent stress values close to yield while orange and light blue stresses between 100 and 200 MPa. The structure around # 77 have different qualities with yield stresses varying in the longitudinal directions, with mild steel (yield stress 235 MPa) mostly aft of #77 and high strength steel (yield stress 315 MPa) forward of #77.

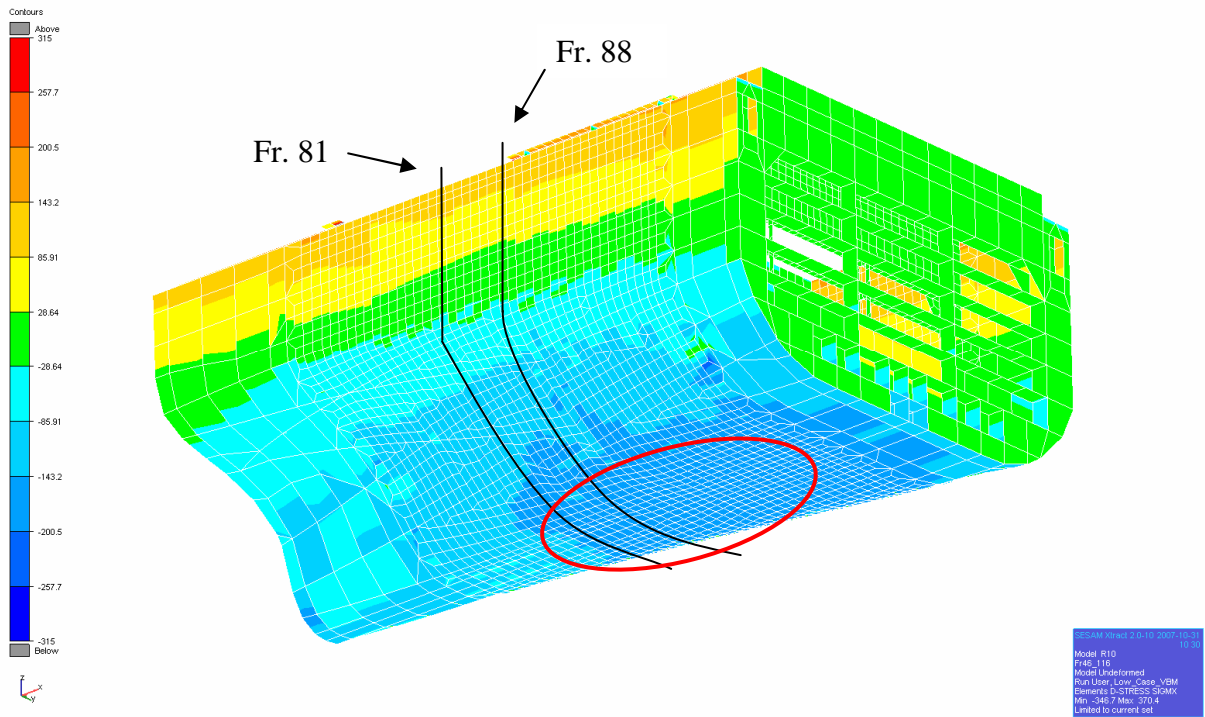


Fig. 5.3 Global FE SESAM: Longitudinal stress # 46 to # 116, bottom view
 (VBM at # 88 = 3300 MNm)

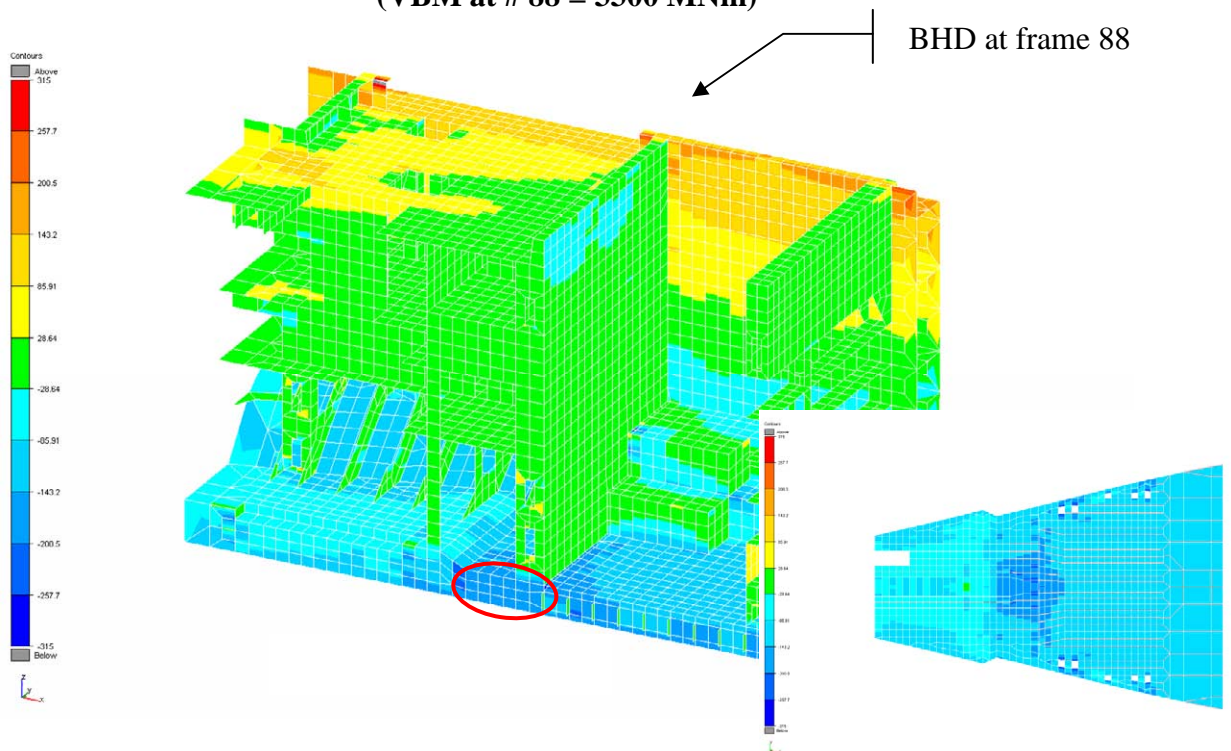


Fig. 5.4 Global FE SESAM: Longitudinal stress # 46 to # 116, internal and tank top view.
 (VBM at # 88 = 3300 MNm)

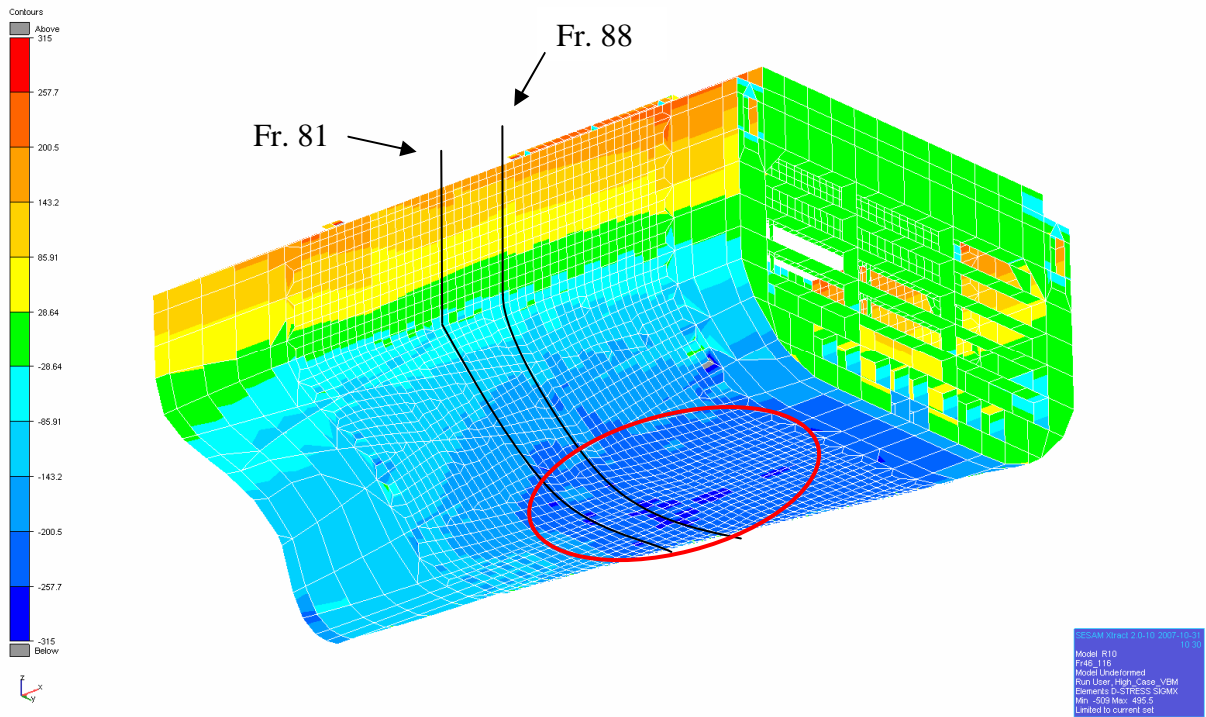


Fig. 5.5 Global FE SESAM: Longitudinal stress # 46 to # 116, bottom view

(VBM at # 88 = 4600 MNm)

BHD at frame 88

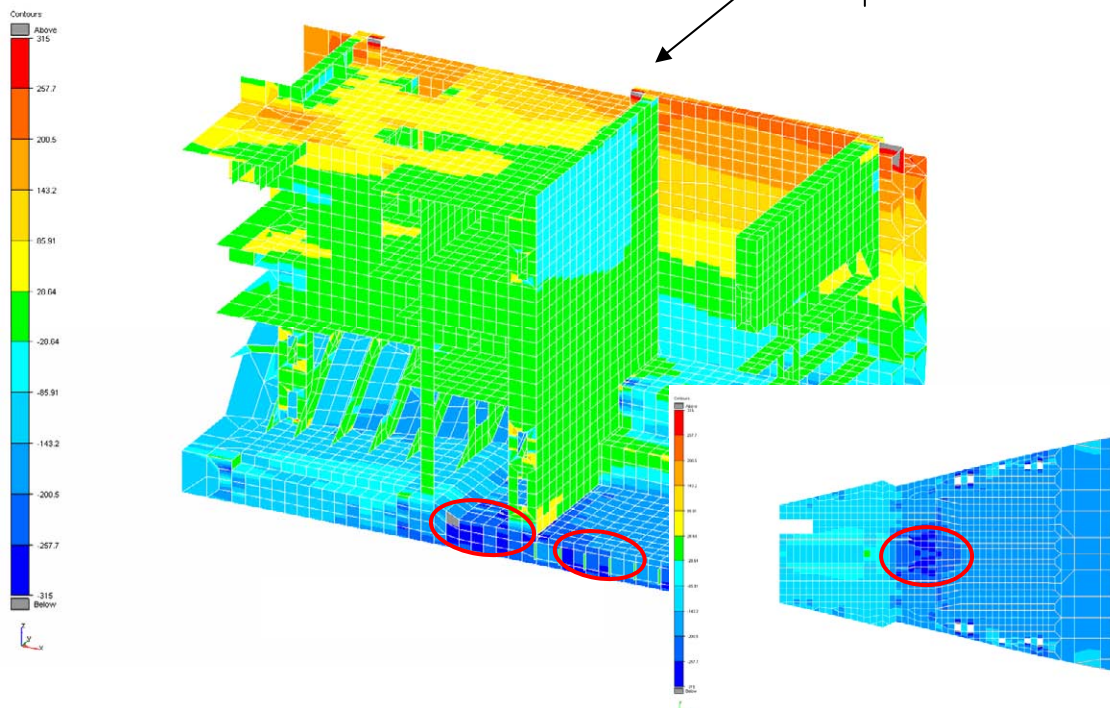


Fig. 5.6 Global FE SESAM: Longitudinal stress # 46 to # 116, internal and tank top view.

(VBM at # 88 = 4600 MNm)

6 NON-LINEAR ANALYSES – COLLAPSE AND FAILURE ASSESSMENTS

6.1 Model description

Linear stress analysis methods are not capable of identifying buckling and material yielding in the structure, effects which are crucial for hull capacity and progressive failure mechanism assessments. Therefore a non-linear stress and capacity model was made by refining the SESAM FE model from Chap. 5. The main change was to remodel to an even finer mesh level the # 78 - # 92 part of the engine room.

The total refined model was imported into the non-linear FE program ABAQUS, ref./3/ and analysed for hull capacity and progressive collapse behaviour. A brief description of this model and the analyses assumptions are given in this section.

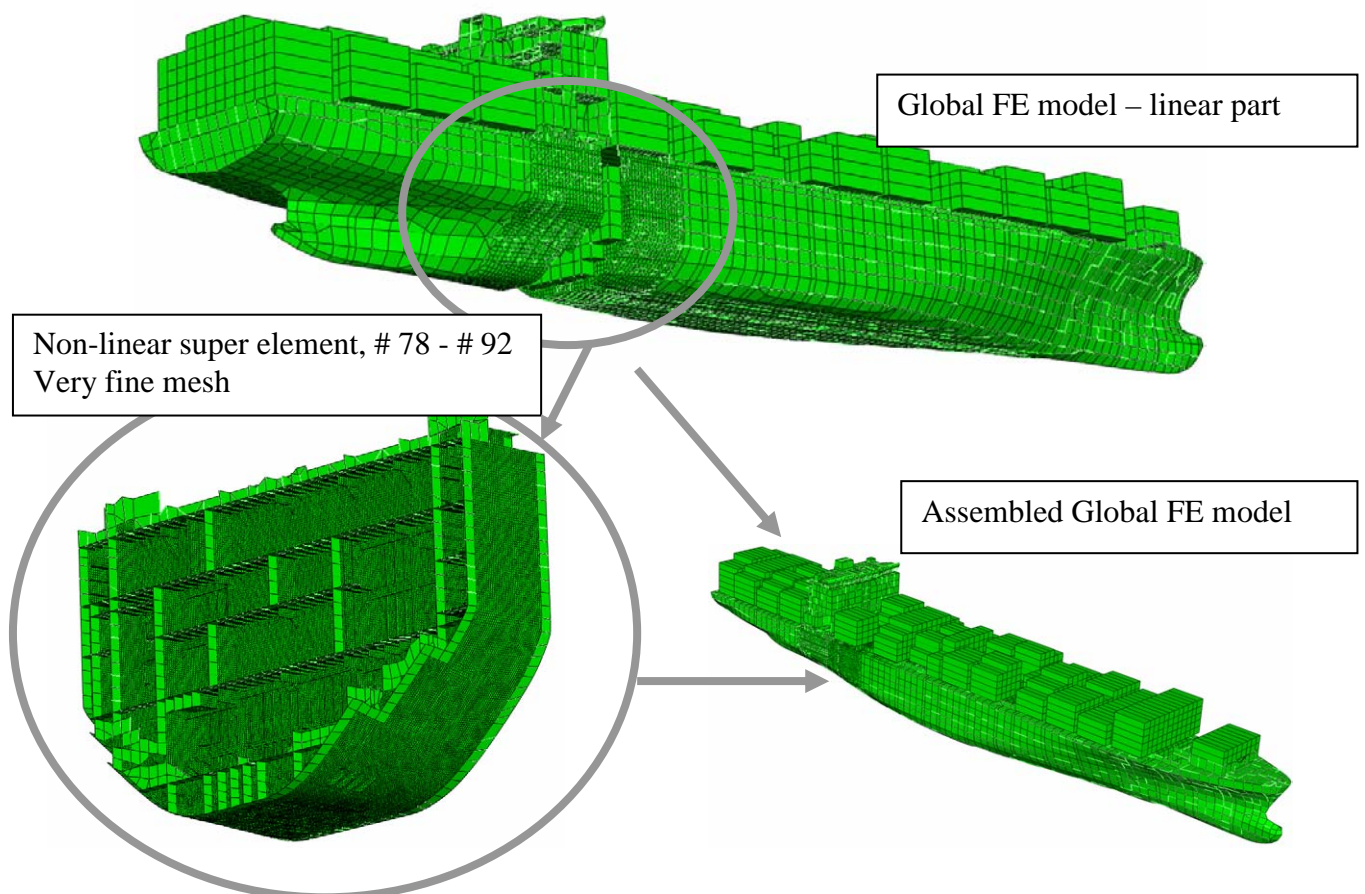


Fig. 6.1 Non-linear super-element with very fine mesh inserted into Global FE model

6.1.1 Mesh density and properties

The global FE model used in this analysis consists of two super-elements:

- A local, very fine mesh super-element representing the area between frame 78 and frame 92. Here both non-linearity in geometry and material behaviour is included. It is referred to as the non-linear super-element.
- A global super-element representing the rest of the vessel. This is constrained to behave linearly elastic and it is referred to as the linear super-element.

The non-linear super-element is modelled using 4-node plate element (ABAQUS, S4) for both plating, stiffeners, girder webs etc. The meshing is very fine with typically

- 5 to 6 elements between stiffeners
- 3 elements across a stiffener height
- quadric element shape is chosen for the most of the structure
- element size is of the order 150 mm
- openings, cut-outs and local secondary stiffeners are modelled in detail

This mesh density is capable of describing very localized buckling and collapse behaviour of plating, stiffeners and girder structures.

The model size is

- non-linear super element; 1.06 mill degrees of freedom (dof)
- total model; 1.22 mill degrees of freedom (dof), linear + non-linear super-element

Fig. 6.2 show the non-linear super-element, while Fig 6.3 and Fig. 6.4 show some close up views of bilge and double bottom parts respectively.

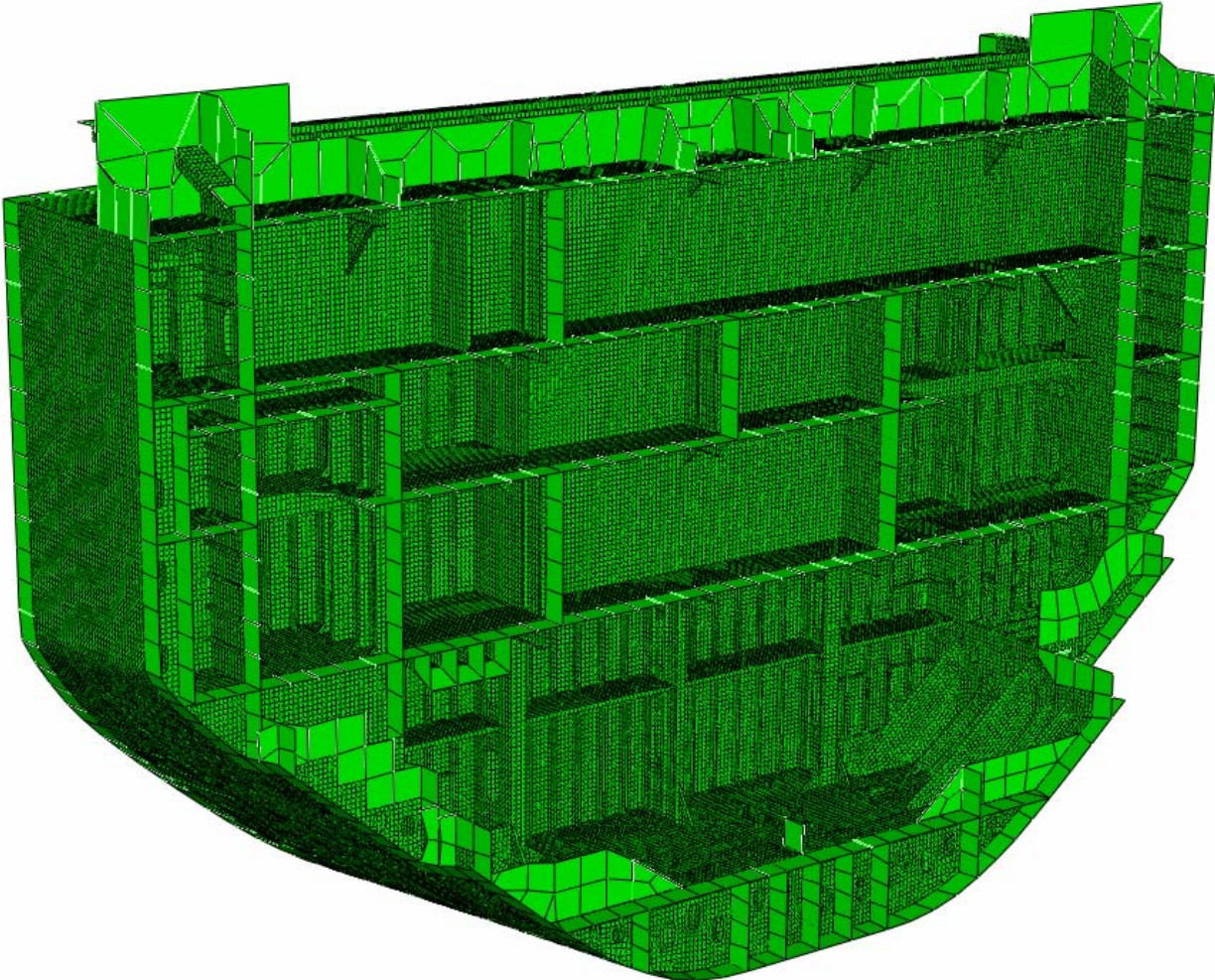


Fig. 6.2 Non-linear super-element; # 79 - # 92

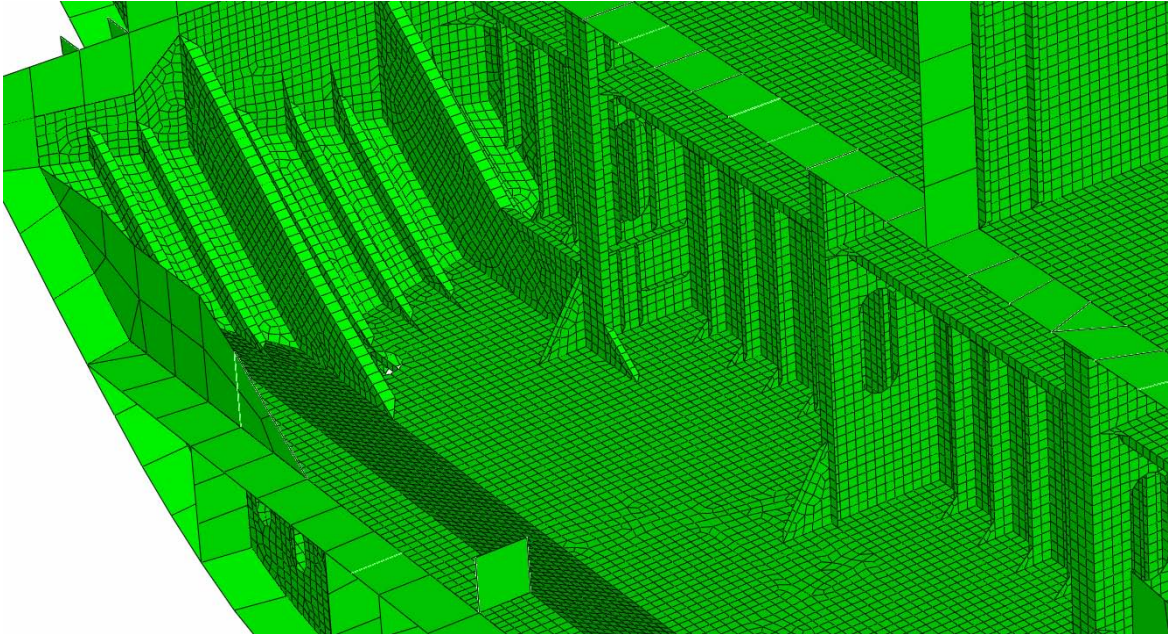


Fig. 6.3 Close up – non-linear super-element, engine room bilge area

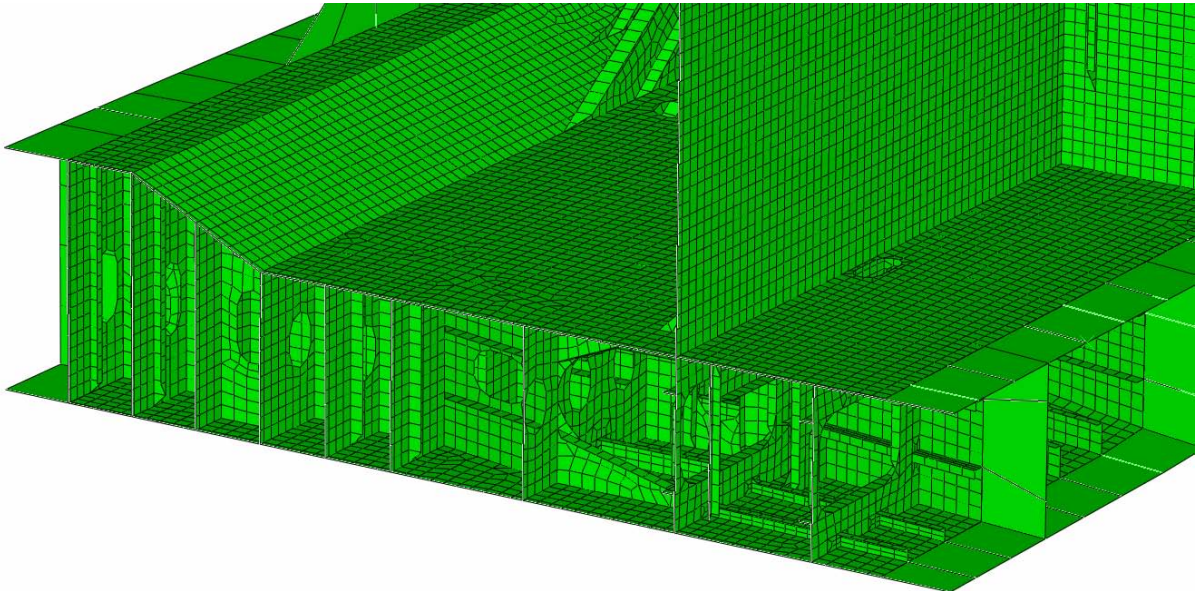


Fig. 6.4 Close up – nonlinear super-element, double bottom area

6.1.2 Geometrical shape imperfections (tolerances)

The assumed pattern of geometrical imperfections is important for non-linear capacity analyses. In particular the imperfections have to be included such that the structure is not prevented from buckling and collapsing into the most critical and detrimental modes.

The imperfection pattern used in the present analyses is shown Fig. 6.5. The pattern is strongly scaled up in this figure (200 times) for illustration purposes. In the non-linear analyses the imperfections are set to be small in order for the structure to reflect a strength and ultimate capacity limit consistent with normal fabrication and tolerance levels.

As seen the pattern is rather harmonic, covering the whole lower part of the model, i.e. the outer bottom, tank top plating and bilge area are all given an evenly distributed slight imperfection pattern.

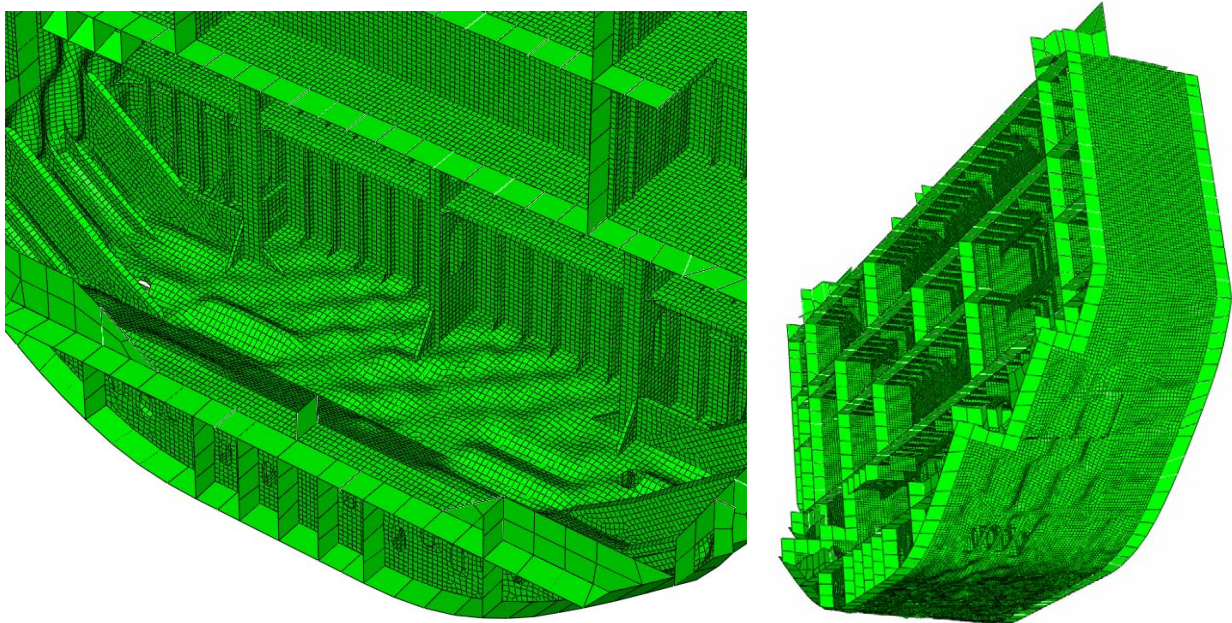


Fig. 6.5. Geometrical imperfections in the non-linear super-element. Imperfection size in figure is scale up 200 times for illustration purposes. Imperfection sizes in the analyses are small reflecting strength consistent with normal fabrication standards

6.1.3 Material properties and yield stress variations

In order to account for non-linear material behaviour, i.e. plastic flow and strain hardening effects, a bi-linear material model has been used.

Moreover, in order to reflect uncertainties and possible yield stress variations in the steel, analyses are carried out for a range of three different sets of material properties:

- Lower 5% quantile yield stress (characteristic yield strength used in Rules)
- Expected, mean value yield stress
- Upper 5% quantile yield stress

The plastic tangent modulus is set to 1000 N/mm^2 for all materials. The tangent module describes the strain hardening properties of the material after material yielding.

The material characteristics are all in line with properties as defined by standard Class rules. The material data and variations used in the analyses are shown in Table 6.1.

This selected range of material characteristics gives the range of ultimate capacity as found using the non-linear ABAQUS hull model.

Table 6.1 Material data and variations in properties

Material	Young's modulus	Poisson ratio	Lower value yield stress	Mean value, yield stress	Upper value, yield stress
Normal Steel	206000	0.3	235	271	307
High strength -32	206000	0.3	315	349	383
High strength -36	206000	0.3	355	394	433

Fig. 6.6 shows the stress-strain curves for the different materials valid for the mean value properties.

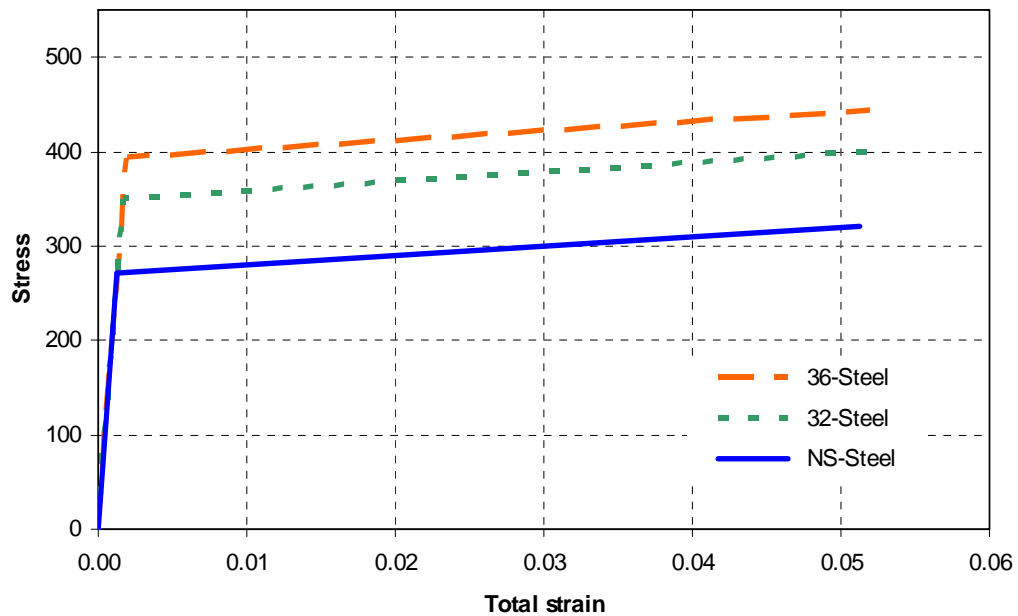


Fig. 6.6 Bi-linear material stress-strain curves, all steel qualities. Curves valid for mean yield stress values

Most of the critical and important load bearing structures within the engine room has a material grade of high strength steel 32. Stress-strain curve for this material is shown in Fig. 6.7, illustrating the range of possible variations according to the Table 6.1 data.

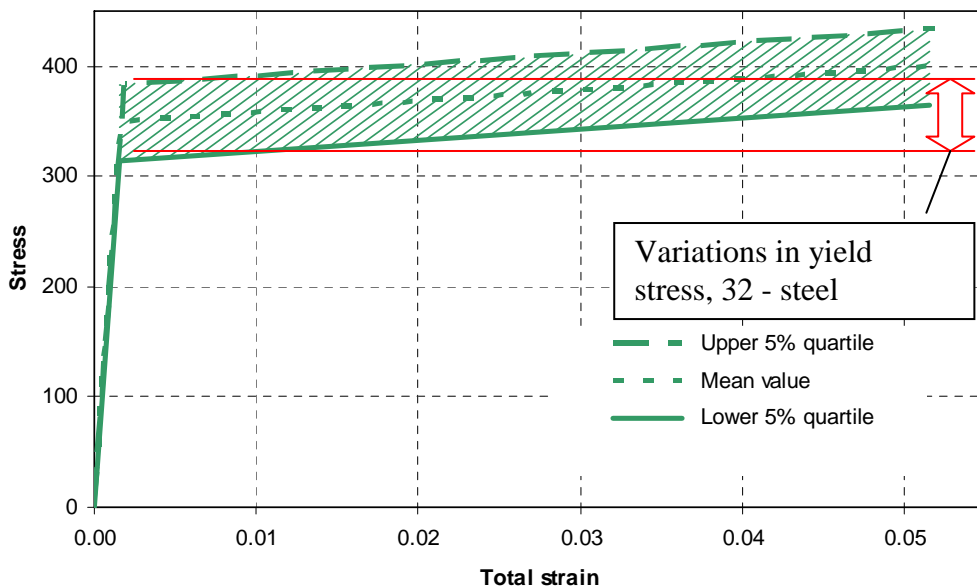


Fig. 6.7 Bi-linear material stress-strain curves for high strength 32 steel with assumed variation range

6.1.4 Load applications

Load transfer:

The loads applied to the ABAQUS super-elements are transferred from the hydrodynamic WASIM analyses and the loading is based on a split into two load categories

- i) still water loading
- ii) loads on the vessel in waves, Fig. 4.1

Hull sea pressures and mass forces representative for both load categories are included.

Load application:

The non-linear analyses are performed in steps as follows (load-history):

- i) First the still-water load set is applied
- ii) Next the wave load set is added
- iii) If global collapse is not achieved as the sum of load i) and ii), the wave load ii) is scaled further until the collapse limit is found. If the collapse limit is lower than the sum of load i) and ii), this will be automatically identified by the procedures used in ABAQUS.

This way of splitting the loads into two sets will take care of the differences in sea pressures and mass forces along the ship length for the still-water and wave load contribution respectively.

6.2 Results

6.2.1 General

The main results from the non-linear ABAQUS analyses are the estimates of the global vertical bending moment and shear load when the hull girder finally collapses. This load level is called the ultimate capacity limit or just capacity limit.

For consistency when comparing acting max loads from Chap. 4.3.5 against the corresponding capacity limit, the vertical bending moment (VBM) at the engine room bulkhead position (# 88) is used. The final capacity results are summarized in Chap. 6.2.2 for the three different material characteristics analysed.

Before the ultimate capacity limit is reached, non-linear effects are observed in the form of initial buckling in the bilge area with subsequent stress redistributions to longitudinal stiff areas (“hard corners”). The development of this progressive failure mechanism is described in more detail in Chap. 6.2.3.

6.2.2 Hull girder capacity

The non-linear relation between vertical moment (VBM) at engine room bulkhead (#88) and the vertical deflection at ship bow is shown in Fig. 6.8. For practical purposes it is the maximum point along the moment-deflection curve that is the most interesting parameter. This max point is the capacity of the structure, called also the ultimate collapse moment of the hull girder (M_u), and it is tabulated separately, see Table 6.2.

Three separate non-linear analyses are run, each corresponding to a selected set of material characteristics according to Table 6.1. All results are shown in Fig. 6.8.

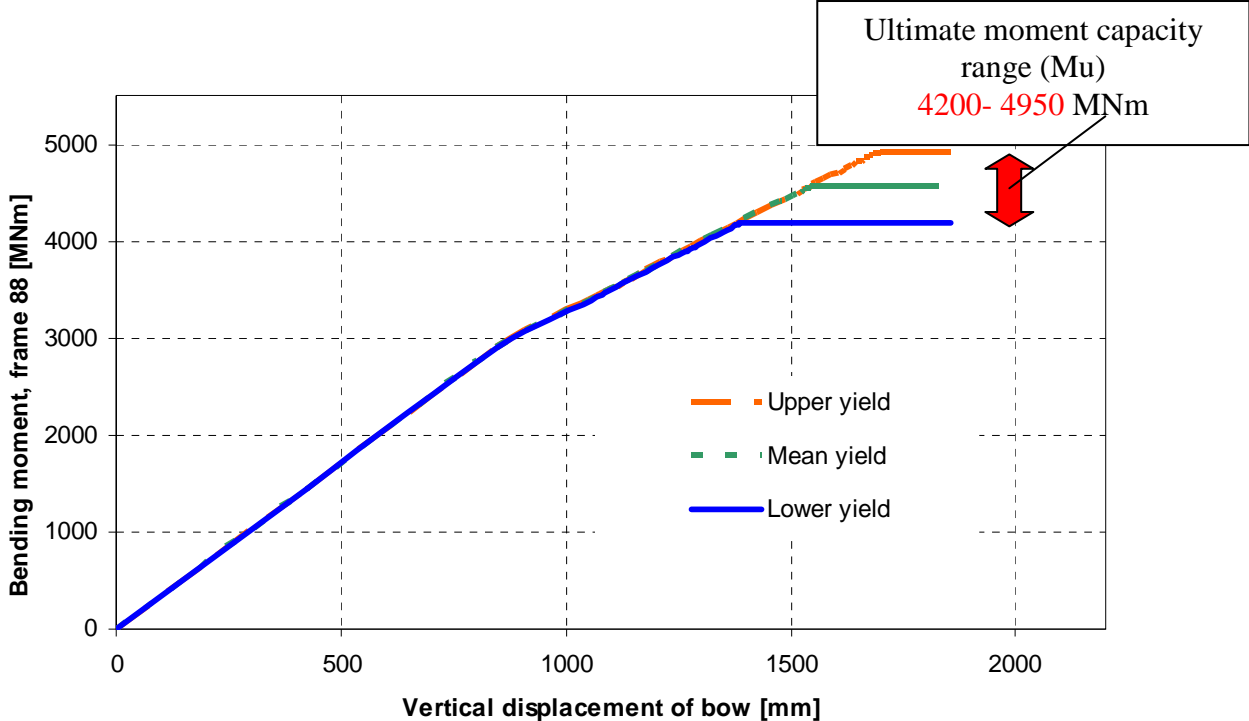


Fig. 6.8 Non-linear moment- displacement relation (Moment at # 88 against vertical bow deflection). Ultimate capacity is the max load indicated for the lower, mean and upper material properties according to Table 6.1.

Table 6.2 gives the ultimate moment capacities summarized for each of the material categories analysed. From this the capacity range is seen to span from 4200 MNm as the lowest level to 4950 MNm as the highest level.

Table 6.2 Results; vertical bending moment (VBM) at # 88 at hull girder collapse

Yield stress used in ABAQUS model acc. to Table 6.1	Vertical moment at #88 at collapse (Mu, MNm)
Lower yield stress	4200
Mean yield stress	4560
Upper yield stress	4950

6.2.3 Hull girder failure mechanism

Associated with the total collapse of the hull girder is the development of a local progressive failure mechanism. The characteristics of this is that it starts with “elastic” buckling in the hull skin plating in the bilge area in way of # 81 to # 88. From here it gradually develops and progress into the bottom, double bottom and up into the ship side. It finally ends up as a localized collapse pattern across the whole hull section, from bottom to ship side, see Fig. 6.9.

The progressive development of the failure mechanism is illustrated in more detail in Fig. 6.10, showing the stepwise development for four subsequent load levels; external and internal view.

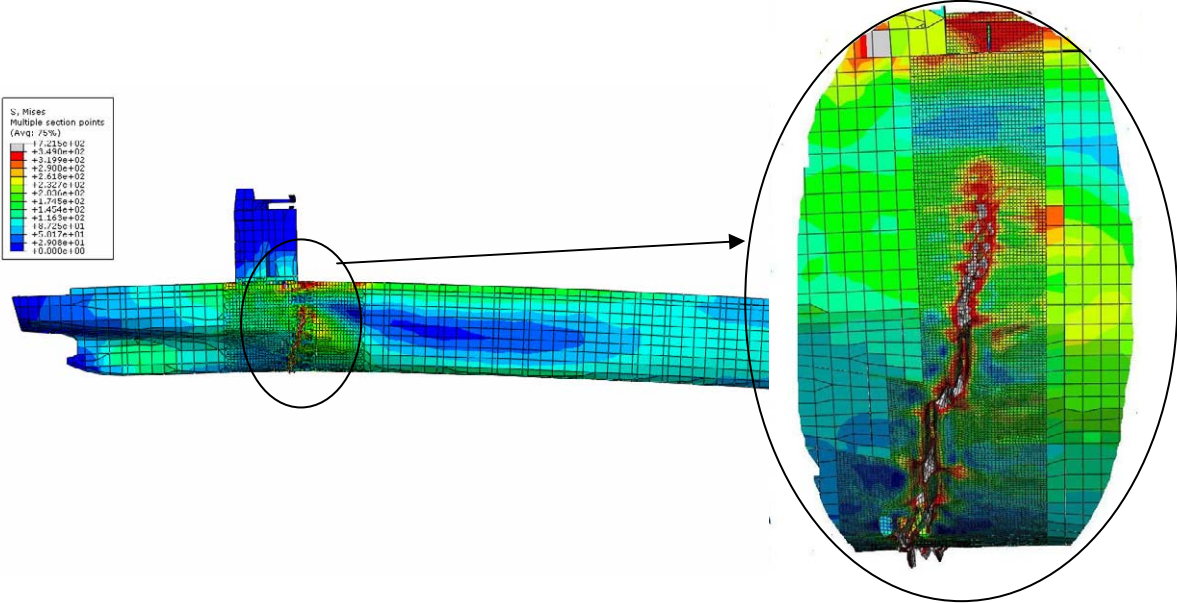


Fig. 6.9 Final failure mechanism as predicted by ABAQUS. Deflections scaled up 5 times for illustration purposes.

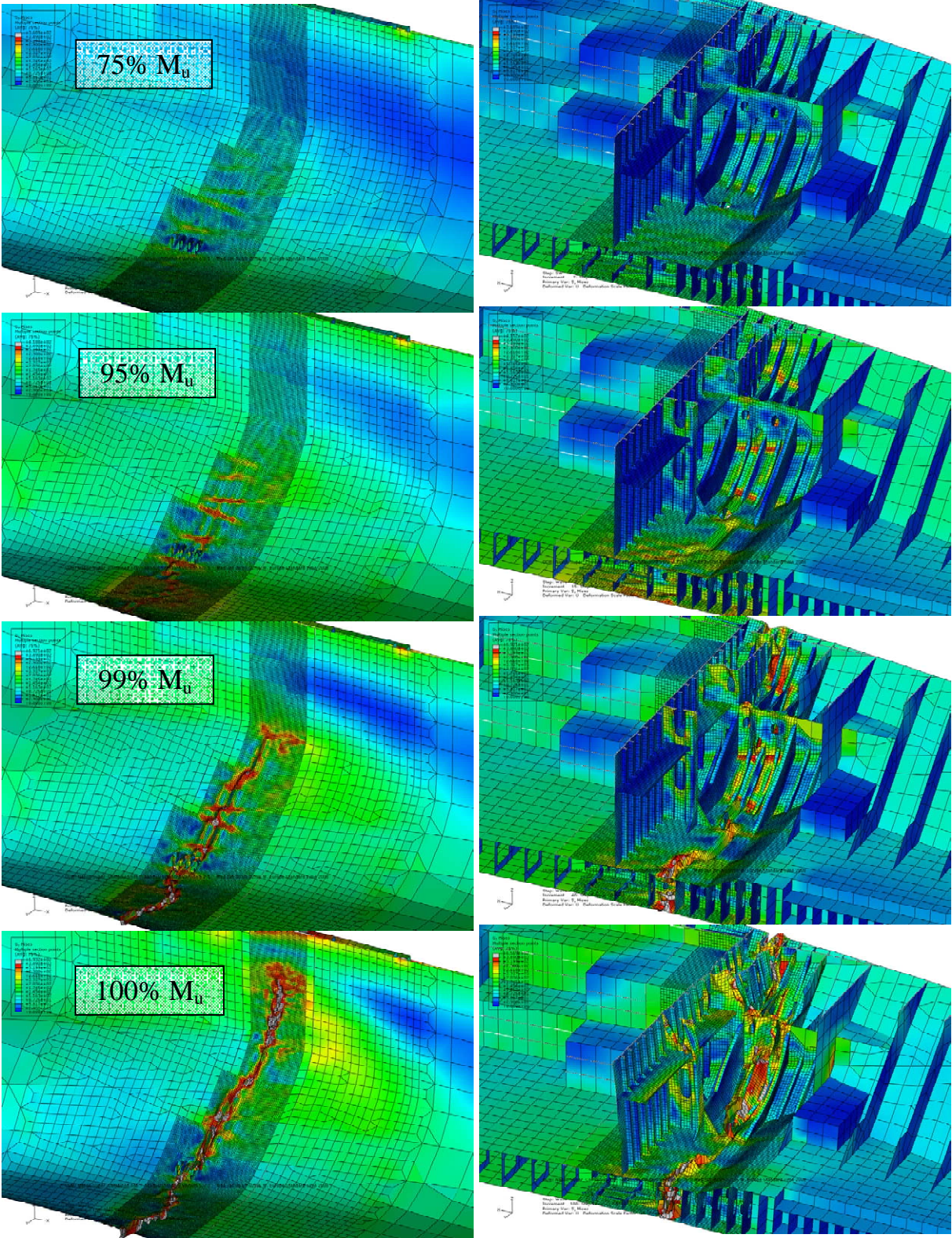


Fig. 6.10 Four stages of progressive collapse, outer (left) and inner structure (right)
Deflections scaled up 5 times for illustration purposes.

7 SUMMARY

7.1 General

The computer analyses demonstrate that a very high vertical hull girder moment, close to or exceeding the corresponding capacity limit, may lead to a type of structural failure between #81 to #88, as is observed on MSC Napoli in open sea. This is evident from a comparison between a photo taken of the vessel's starboard side, before it is beached with the failure visible, and a computer simulation image of the same area, see Fig. 7.1. This is further supported by diving surveys while beached and also later from surveys of the forward part in dry dock.

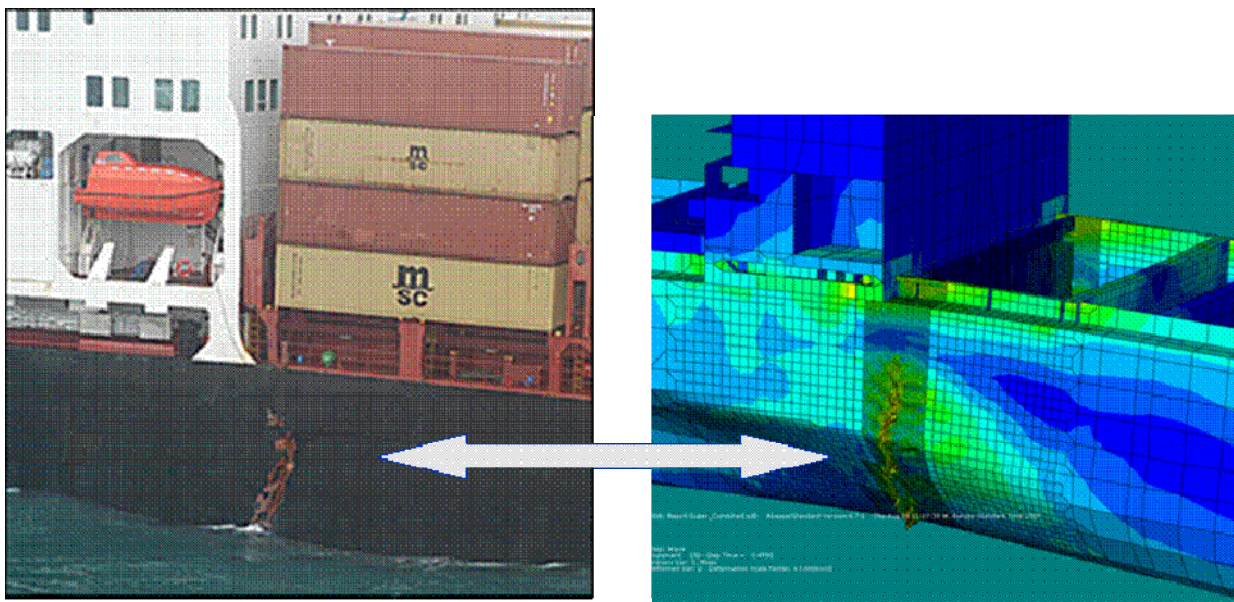


Fig. 7.1 Comparison of real life failure mode with computer simulations (ABAQUS FE model)

(with permission from Gargolaw)

Given the assumptions and uncertainties as described earlier in this report, the computer analyses carried out and documented herein indicate that the total hull girder loads in way of the engine room area may have been on the limit or have exceeded the corresponding hull capacity for MSC Napoli, see Fig. 7.2.

It is also documented that the overlap in load and capacity is very narrow indicating that such a failure scenario has a very low probability of occurrence for the assumed severe sea states.

By screening available wave statistic relevant for the English Channel during the last years it can be concluded that the assumed severe sea states are very rare. This reflects a very low probability for such events to take place in the future.

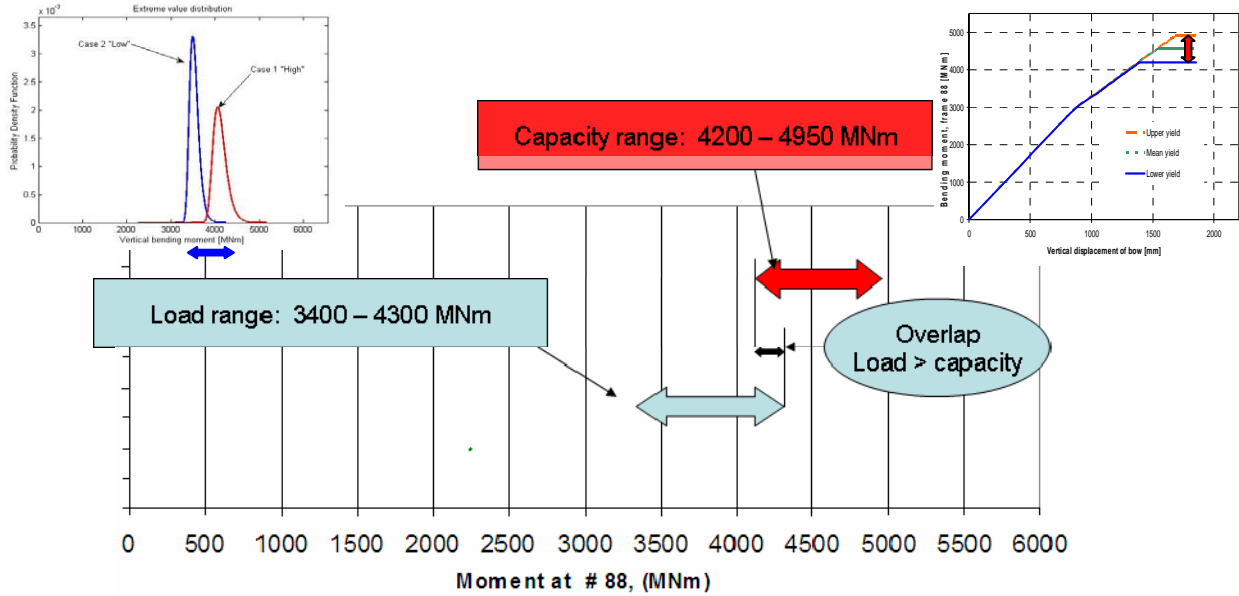


Fig. 7.2 Calculated load and capacity ranges with overlap comparison (no whipping effects). Vertical bending moments (VBM) at engine room bulkhead #88

7.2 Discussion

The non-linear FE computer analyses (ABAQUS) document a localized plate buckling mechanism developing between # 81 and # 88 across the whole ship section, i.e. in the bottom structure as well as far up into the shipside. Such large plate bending and folding deformations lead to large plastic strains also in a tension mode. This may lead to sudden ductile plate fracture and cracking with subsequent water ingress and compartment flooding as a consequence.

The exact nature and sequence of the structural failure and plate fracture taking place is difficult to judge, but it is a possibility that not only one severe wave but several subsequent high waves hit the MSC Napoli. This typically will lead to a loading, unloading and reloading again as the ship move through the waves. This again gives locally a plastic straining of the hull plating at

one instant, and then in the next moment having a strain relief followed by a new large plastic straining. Such hysteresis behaviour in the large plastic strain region may lead to plate fracture and locally open up large cracks. However, due to the large and localized plate bending deformations initiated from buckling, only one severe wave may be enough to strain the hull plating beyond its fracture limit and thereby generate rupture and large cracks.

A major uncertainty is linked to the wave response characteristics, i.e. the wave response could have had a whipping (vibration) contribution on top of the regular wave load, the former being the result of the vessel slamming into a severe wave train. However, as discussed in Chapter 4.3.4 the whipping effects for the MSC Napoli is not assessed explicitly as no consistent analyses tools are available. Accordingly, whipping effects may have been a triggering factor, but they are of an unknown magnitude and may not have been decisive for the incident.

REFERENCES

- /1/ MV MSC Napoli, W05 Spl. TD Voy. 27a - Departure from Antwerp to Sines, Date 16/01/07, MSC. (Onboard Loading Computer) (MAIB 98%)
- /2/ DNV SESAM User Manuals 2007 (FE and WASIM)
- /3/ ABAQUS User Manual 2007, version 6.7-1
- /4/ NAPA User Manual 2006, version 2006.2

- o0o -